

A LATENT PROCESS MODEL FOR MONITORING PROGRESS TOWARDS HARD-TO-MEASURE TARGETS, WITH APPLICATIONS TO MENTAL HEALTH AND ONLINE EDUCATIONAL ASSESSMENTS

BY MINJEONG JEON AND MICHAEL SCHWEINBERGER

University of California, Los Angeles and Penn State University

The recent shift to remote learning and work has aggravated long-standing problems, such as the problem of monitoring the mental health of individuals and the progress of students towards learning targets. We introduce a novel latent process model with a view to monitoring the progress of individuals towards a hard-to-measure target of interest, measured by a set of variables. The latent process model is based on the idea of embedding both individuals and variables measuring progress towards the target of interest in a shared metric space, interpreted as an interaction map that captures interactions between individuals and variables. The fact that individuals are embedded in the same metric space as the target helps assess the progress of individuals towards the target. We pursue a Bayesian approach and present simulation results along with applications to mental health and online educational assessments.

1. Introduction. The recent shift to remote learning and work has aggravated long-standing problems, such as the problem of monitoring the mental health of individuals (e.g., [Daly et al., 2020](#); [Holmes et al., 2020](#)) and the progress of students towards learning targets (e.g., [Engzell et al., 2021](#); [Kuhfeld and et al., 2020](#); [Bansak and Starr, 2021](#)).

We introduce a novel approach to monitoring the progress of individuals towards a hard-to-measure target of interest. Examples are measuring the progress of individuals with mental health problems or the progress of students towards learning targets. Both examples have in common that there is a target of interest (e.g., improving mental health or the understanding of mathematical concepts) and measuring progress towards the target is more challenging than measuring changes in physical quantities (e.g., temperature) or medical conditions (e.g., cholesterol levels), but a set of variables is available for measuring progress towards the target. If, e.g., the goal is to monitor the progress of students towards learning targets, measurements can be collected by paper-and-pencil or computer-assisted educational assessments, whereas progress in terms of mental health can be monitored by collecting data on mental well-being by using surveys along with physical measurements related to stress by using wearable devices.

We propose a novel latent process model with a view to monitoring the progress of individuals towards a target of interest, measured by a set of variables. The latent process model is based on the idea of embedding both individuals and variables measuring progress towards the target of interest in a shared metric space and can be considered as a longitudinal extension of the [Jeon et al. \(2021\)](#) model. The fact that individuals are embedded in the same metric space as the target helps capture

*Equal contributions.

Keywords and phrases: latent space models, measurement models, item response models

- interactions between individuals and variables arising from unobserved variables, such as cultural background, upbringing, and mentoring of students, which may affect responses;
- whether individuals make progress towards the target;
- how much progress individuals make towards the target;
- how much more progress individuals can make in the future.

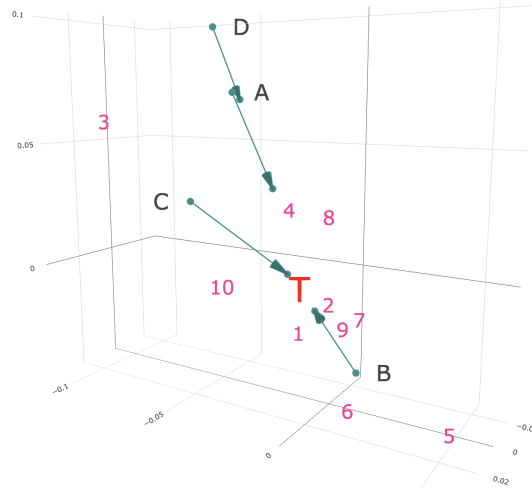


FIG 1. *Mental health: An interaction map (\mathbb{M}, d) with $\mathbb{M} := \mathbb{R}^3$ and $d(\mathbf{a}, \mathbf{b}) := \|\mathbf{a} - \mathbf{b}\|_2$ ($\mathbf{a} \in \mathbb{M}$, $\mathbf{b} \in \mathbb{M}$) shows the progress of selected mothers A, B, C, D in low-income communities towards the target of interest \mathcal{T} (improving mental health), measured by items $1, \dots, 10$ (questions about depression). The interaction map is estimated by a Bayesian approach to the proposed latent process model. The interaction map reveals interactions between individuals (mothers) and items (questions about depression): e.g., item 5 deviates from the bulk of the items, and mother B is closest to item 5. It turns out that mother B agreed with item 5 at the first assessment (“feeling hopeful”), whereas mothers A, C, D did not. In addition to revealing interactions, the interaction map suggests that mothers B and C have made strides towards improving mental health, while mothers A and D may need to make more progress.*

1.1. *Motivating example.* To demonstrate the proposed latent process model, we assess the progress of 257 mothers with infants in low-income communities towards improving mental health. The data are taken from Santos et al. (2018) and are described in more detail in Section 5.

Figure 1 presents an interaction map, based on a Bayesian approach to the proposed latent process model. The interaction map embeds individuals (mothers) and items (questions about depression) into Euclidean space (\mathbb{M}, d) . The interaction map offers at least three insights:

- Out of the 10 items used to assess the mental health of the 257 mothers, some of the items (e.g., items 3 and 5) deviate from the bulk of the items.
- There are interactions between individuals (mothers) and items (questions about depression): e.g., mother B is closest to item 5. It turns out that mother B agreed with item 5 at the first assessment (“feeling hopeful”), whereas mothers $A, C,$ and D did not.
- Mothers B and C have made strides towards improving mental health, whereas mothers A and D may need to make more progress in the future.

Figure 2 clarifies that the progress of mother A is unclear, but confirms the conclusions regarding mothers $B, C,$ and D . We describe the results in more detail in Section 5.

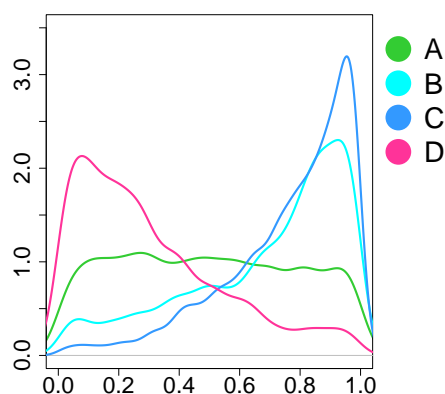


FIG 2. Mental health: Marginal posteriors of the rates of progress $\lambda_A, \lambda_B, \lambda_C, \lambda_D \in [0, 1]$ of mothers A, B, C, D towards target \mathcal{T} (improving mental health). The progress of mother A is unclear, but the marginal posteriors of the rates of progress λ_B and λ_C of mothers B and C have modes close to 1, confirming that mothers B and C have made strides towards improving mental health. By contrast, the marginal posterior of the rate of progress λ_D of mother D has a mode close to 0, underscoring that mother D may need additional assistance.

1.2. *Existing approaches.* A classic approach to longitudinal educational assessments is based on Andersen's (1985) model. Andersen's (1985) model assumes that binary responses $Y_{i,j,t} \in \{0, 1\}$ are independent Bernoulli($\mu_{i,j,t}$) random variables with $\text{logit}(\mu_{i,j,t}) := \alpha_{i,t} + \beta_j$, where $\alpha_{i,t} \in \mathbb{R}$ can be interpreted as the ability of student i at time t and $\beta_j \in \mathbb{R}$ can be interpreted as the easiness of item j . Based on Andersen's (1985) model, the progress of student i between time $t = 1$ and $t = 2$ can be quantified by $\alpha_{i,2} - \alpha_{i,1}$. Embretson (1991) reparameterized Andersen's (1985) model by modeling changes in abilities via $\delta_i := \alpha_{i,2} - \alpha_{i,1}$. Andersen's (1985) model has been extended with a view to capturing temporal dependence (e.g., Cai, 2010), and addressing multiple learning topics at each time point (e.g., Wang and Nydick, 2020; Huang, 2015). Other approaches model a linear change in abilities as a function of time (e.g., Pastor and Beretvas, 2006; Wilson et al., 2012) and incorporate first-order autoregressive structure (Jeon and Rabe-Hesketh, 2016; Segawa, 2005).

In summary, Andersen's (1985) model and its extensions help educators estimate the progress of students i by estimating differences in abilities $\alpha_{i,2} - \alpha_{i,1}$ (model estimation). That said, these models do not help educators determine whether students make progress at all (model selection), which would enable educators identify students who need more support than others. In addition, these models assume that all students i with the same ability $\alpha_{i,t}$ have the same response probability for all items j with the same easiness β_j . Such assumptions may well be violated in applications, because some students i with the same ability $\alpha_{i,t}$ may respond to items j with the same easiness β_j differently, owing to unobserved variables such as cultural background, upbringing, and mentoring. By contrast, the proposed latent process captures interactions among individuals (students) and variables (items) and provides a visual interaction map to reveal such interactions, in addition to helping assess whether individuals make progress; how much progress individuals make; and how much more progress individuals can make in the future.

A more detailed comparison of the proposed latent process model and Andersen's (1985) model

can be found in Section 2.4.

1.3. *Outline.* We introduce the proposed latent process model in Section 2 and outline a Bayesian approach to statistical inference in Section 3. Simulation results and applications can be found in Sections 4, 5, and 6, respectively.

2. Latent process model. We consider responses $Y_{i,j,t} \in \mathcal{Y}_{i,j,t}$ of individuals $i \in \{1, \dots, n\}$ ($n \geq 1$) to variables $j \in \{1, \dots, p\}$ ($p \geq 1$) at times $t \in \{1, \dots, T\}$ ($T \geq 2$). To accommodate data from multiple sources (e.g., self-reported mental health assessments collected by surveys and physical measurements related to stress collected by wearable devices), we allow responses $Y_{i,j,t}$ to be binary ($\mathcal{Y}_{i,j,t} = \{0, 1\}$), count-valued ($\mathcal{Y}_{i,j,t} = \{0, 1, \dots\}$), or real-valued ($\mathcal{Y}_{i,j,t} = \mathbb{R}$).

To monitor the progress of individuals towards a target of interest \mathcal{T} , we assume that the individuals and the variables measuring progress towards target \mathcal{T} have positions in a shared metric space (\mathbb{M}, d) , consisting of a set \mathbb{M} and a distance function $d : \mathbb{M}^2 \mapsto [0, +\infty)$. We assume that the set \mathbb{M} is convex and allow the metric space (\mathbb{M}, d) to be Euclidean or non-Euclidean. In the domain of statistical network analysis (Hunter et al., 2012; Smith et al., 2019), two broad classes of latent space models can be distinguished, based on the geometry of the underlying metric space: Euclidean latent space models (Hoff et al., 2002) and latent models with intrinsic hierarchical structure, based on ultrametric space (Schweinberger and Snijders, 2003) or hyperbolic space (Krioukov et al., 2010). The proposed probabilistic framework can accommodate these and other metric spaces. A discussion of the non-trivial issue of choosing the geometry of the metric space (\mathbb{M}, d) can be found in Section 2.3. Given a metric space (\mathbb{M}, d) , we assume that individuals i have positions $\mathbf{a}_{i,t} \in \mathbb{M}$ at time t and move towards the target of interest $\mathcal{T} \in \mathbb{M}$, measured by variables j with positions $\mathbf{b}_j \in \mathbb{M}$. The position of the target \mathcal{T} is assumed to be time-invariant. It is possible to extend the proposed latent process model to time-varying targets, provided that the data at hand warrant the resulting increase in model complexity, but we do not consider such extensions here.

We assume that the responses $Y_{i,j,t} \in \mathcal{Y}_{i,j,t}$ are independent conditional on the positions $\mathbf{a}_{i,t}$ of individuals i at time t and the positions \mathbf{b}_j of variables j measuring progress towards target \mathcal{T} , and are distributed as

$$Y_{i,j,t} \mid \boldsymbol{\theta}, \mathbf{a}_{i,t}, \mathbf{b}_j \stackrel{\text{ind}}{\sim} \mathbb{P}_{\boldsymbol{\theta}, \mathbf{a}_{i,t}, \mathbf{b}_j},$$

where $\mathbb{P}_{\boldsymbol{\theta}, \mathbf{a}_{i,t}, \mathbf{b}_j}$ is a probability distribution with support $\mathcal{Y}_{i,j,t}$ and $\boldsymbol{\theta} \in \Theta$ is a vector of parameters.

We divide the description of the probabilistic framework into

- the data model: the model that generates the responses $Y_{i,j,t}$ conditional on the positions $\mathbf{a}_{i,t}$ of individuals i at time t and the positions \mathbf{b}_j of variables j measuring progress towards the target of interest \mathcal{T} (Section 2.1);
- the process model: the process that determines whether and how much progress individuals i make towards the target of interest \mathcal{T} (Section 2.2).

The non-trivial issue of selecting the geometry of the metric space is discussed in Section 2.3. We compare the proposed latent process model to Andersen's (1985) classic model in Section 2.4 and mention other possible approaches to assessing progress in Section 2.5. Priors are reviewed in Section 2.6, and identifiability issues are discussed in Section 2.7.

2.1. *Data model.* The data model describes how the responses $Y_{i,j,t}$ are generated conditional on the positions $\mathbf{a}_{i,t}$ of individuals i at time t and the positions \mathbf{b}_j of variables j measuring progress towards the target of interest \mathcal{T} .

To leverage data from multiple sources (e.g., binary, count-, and real-valued responses), we assume that the responses $Y_{i,j,t}$ are generated by generalized linear models (Sundberg, 2019; Efron, 2022). Let

$$\mu_{i,j,t}(\boldsymbol{\theta}, \mathbf{a}_{i,t}, \mathbf{b}_j) := \mathbb{E}_{\boldsymbol{\theta}, \mathbf{a}_{i,t}, \mathbf{b}_j} Y_{i,j,t}$$

be the mean response of individual i to variable j at time t and $\eta_{i,j,t}$ be a link function, which links the mean response $\mu_{i,j,t}$ to a linear predictor:

$$\eta_{i,j,t}(\mu_{i,j,t}(\boldsymbol{\theta}, \mathbf{a}_{i,t}, \mathbf{b}_j)) := \begin{cases} \alpha_i + \beta_j - \gamma d(\mathbf{a}_{i,t}, \mathbf{b}_j) & \text{if } t = 1 \\ \alpha_i + \beta_j - \gamma d(\mathbf{a}_{i,t}, \mathcal{T}) & \text{if } t = 2, \dots, T, \end{cases}$$

where $\mathcal{T} := (1/p) \sum_{j=1}^p \mathbf{b}_j$ is the target of interest, measured by variables j with positions \mathbf{b}_j , and $\boldsymbol{\theta} \in \Theta$ is the vector of weights $\alpha_i \in \mathbb{R}$ ($i = 1, \dots, n$), $\beta_j \in \mathbb{R}$ ($j = 1, \dots, p$), and $\gamma \in [0, +\infty)$. The fact that the weights α_i and β_j do not depend on time t implies that the distance term $d(\mathbf{a}_{i,t}, \mathcal{T})$ captures the progress of individual i towards target \mathcal{T} .

The proposed data model can be viewed as an extension of the Rasch (1960) model and the Jeon et al. (2021) model to longitudinal data. The Rasch (1960) model and the Jeon et al. (2021) model consider binary responses $Y_{i,j} \in \{0, 1\}$ observed at $T = 1$ time point and assume that $Y_{i,j} | \mu_{i,j} \stackrel{\text{ind}}{\sim} \text{Bernoulli}(\mu_{i,j})$, where $\text{logit}(\mu_{i,j}) := \alpha_i + \beta_j$ (Rasch, 1960) and $\text{logit}(\mu_{i,j}) := \alpha_i + \beta_j - \gamma d(\mathbf{a}_i, \mathbf{b}_j)$ (Jeon et al., 2021). The proposed data model can be viewed as an extension of these models to binary and non-binary responses $Y_{i,j,t}$ observed at $T \geq 2$ time points $t \in \{1, \dots, T\}$, and reduces to

- the Rasch (1960) model when binary responses $Y_{i,j} \in \{0, 1\}$ are observed at $T = 1$ time point, the link function is the logit link, and $\gamma = 0$;
- the Jeon et al. (2021) model when binary responses $Y_{i,j} \in \{0, 1\}$ are observed at $T = 1$ time point, the link function is the logit link, and $\gamma \in [0, +\infty)$.

As a result, the proposed data model inherits the advantages of the Jeon et al. (2021) model: e.g., in educational assessments,

- α_i can be interpreted as the ability of student i ;
- β_j can be interpreted as the easiness of item j ;
- the metric space (\mathbb{M}, d) can be interpreted as an interaction map that captures interactions between students i and items j .

It is worth noting that the latent space should not be interpreted as an ability map, because the ability of student i is captured by α_i . Instead, the latent space should be interpreted as an interaction map, capturing interactions between students i and items j : e.g., a large distance between student i and item j indicates that the mean response of student i to item j is lower than would be expected based on the ability α_i of student i and the easiness β_j of item j .

In addition to inheriting the advantages of the Jeon et al. (2021) model, the proposed data model helps assess

- whether student i makes progress towards learning target \mathcal{T} , based on changes of the distance $d(\mathbf{a}_{i,t}, \mathcal{T})$ as a function of time t ;
- how much progress student i makes towards learning target \mathcal{T} , based on changes of the distance $d(\mathbf{a}_{i,t}, \mathcal{T})$, and how much uncertainty is associated with such assessments;
- how much more progress student i can make in the future.

2.2. *Process model.* The process model determines whether and how much progress individuals i make towards the target of interest \mathcal{T} . The process model assumes that a metric space (\mathbb{M}, d) has been chosen. We discuss the non-trivial issue of selecting the geometry of the metric space (\mathbb{M}, d) in Section 2.3 and review special cases of metric spaces in Section 2.2.1 (normed vector spaces), Section 2.2.2 (Euclidean space), and 2.2.3 (hyperbolic space).

The latent process model assumes that the variables j measuring progress towards target \mathcal{T} are located at positions

$$\mathbf{b}_j \stackrel{\text{iid}}{\sim} G,$$

where G is a distribution with support \mathbb{M} . The target \mathcal{T} is defined as $\mathcal{T} := (1/p) \sum_{j=1}^p \mathbf{b}_j$.

The positions $\mathbf{a}_{i,t}$ of individuals i at time t are generated as follows. First, the position $\mathbf{a}_{i,1}$ of individual i at time $t = 1$ is generated by sampling

$$\mathbf{a}_{i,1} \stackrel{\text{iid}}{\sim} H,$$

where H is a distribution with support \mathbb{M} . The position $\mathbf{a}_{i,t}$ of individual i at time $t \in \{2, \dots, T\}$ is a convex combination of i 's position $\mathbf{a}_{i,t-1}$ at time $t-1$ and the target's position $\mathcal{T} := (1/p) \sum_{j=1}^p \mathbf{b}_j$:

$$(2.1) \quad \mathbf{a}_{i,t} := (1 - \lambda_{i,t}) \mathbf{a}_{i,t-1} + \lambda_{i,t} \mathcal{T},$$

where $\mathbf{a}_{i,t} \in \mathbb{M}$ provided that $\mathbf{a}_{i,t-1} \in \mathbb{M}$ and $\mathcal{T} \in \mathbb{M}$, because the set \mathbb{M} is convex. The quantity $\lambda_{i,t} \in [0, 1]$ can be interpreted as the rate of progress of individual i towards target \mathcal{T} between time $t-1$ and t . In other words, if individual i makes progress, i moves towards target \mathcal{T} on the shortest path between $\mathbf{a}_{i,t-1}$ and \mathcal{T} . A random term can be added to the right-hand side of (2.1) to allow individuals i to deviate from the shortest path between $\mathbf{a}_{i,t-1}$ and \mathcal{T} . That said, we prefer to keep the model simple and do not consider deviations of individuals i from the shortest path between $\mathbf{a}_{i,t-1}$ and \mathcal{T} , because the moves of individuals i in \mathbb{M} are unobserved. Covariates can be incorporated into the rates of progress $\lambda_{i,t}$ of individuals i between time $t-1$ and t by using a suitable link function.

2.2.1. *Special cases.* In general, the process model makes two assumptions. First, the set \mathbb{M} is convex, so that the positions $\mathbf{a}_{i,t} := (1 - \lambda_{i,t}) \mathbf{a}_{i,t-1} + \lambda_{i,t} \mathcal{T}$ of individuals i at time t are contained in the set \mathbb{M} , provided that $\mathbf{a}_{i,t-1} \in \mathbb{M}$ and $\mathcal{T} \in \mathbb{M}$. Second, the set \mathbb{M} is equipped with a distance function d , so that the distances between individuals i and variables j measuring progress towards target \mathcal{T} can be quantified.

Despite the fact that the process model—at least in its most general form—does not require more than two assumptions, the interpretation and application of the process model is facilitated by additional assumptions. For example, the interpretation of the process model is facilitated if the set \mathbb{M} is endowed with a norm $\|\cdot\|$ (Euclidean or non-Euclidean) and $d(\mathbf{a}_{i,t}, \mathcal{T}) := \|\mathbf{a}_{i,t} - \mathcal{T}\|$, because the distance $d(\mathbf{a}_{i,t}, \mathcal{T})$ can then be expressed as a function of the distance $d(\mathbf{a}_{i,t-1}, \mathcal{T})$:

$$d(\mathbf{a}_{i,t}, \mathcal{T}) = \|((1 - \lambda_{i,t}) \mathbf{a}_{i,t-1} + \lambda_{i,t} \mathcal{T}) - \mathcal{T}\| = (1 - \lambda_{i,t}) d(\mathbf{a}_{i,t-1}, \mathcal{T}).$$

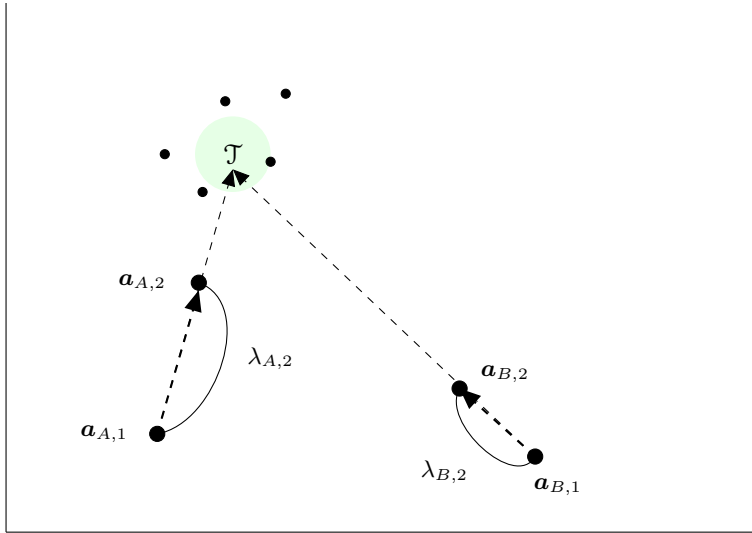


FIG 2. Interaction map: Two individuals A and B with positions $\mathbf{a}_{A,1}$ and $\mathbf{a}_{B,1}$ at time 1 and positions $\mathbf{a}_{A,2}$ and $\mathbf{a}_{B,2}$ at time 2 make progress towards a target of interest $\mathcal{T} := (1/p) \sum_{j=1}^p \mathbf{b}_j$, measured by variables j with positions \mathbf{b}_j (unlabeled points). The interaction map represents interactions between individuals and variables along with the progress of individuals towards target \mathcal{T} . The rates of progress $\lambda_{A,2}$ and $\lambda_{B,2}$ determine how much the distances of A and B to target \mathcal{T} are reduced between time 1 and 2, respectively.

As a consequence, the rate of progress $\lambda_{i,t}$ of individual i between time $t-1$ and t can be expressed as a function of the distances $d(\mathbf{a}_{i,t-1}, \mathcal{T})$ and $d(\mathbf{a}_{i,t}, \mathcal{T})$:

$$\lambda_{i,t} = 1 - \frac{d(\mathbf{a}_{i,t}, \mathcal{T})}{d(\mathbf{a}_{i,t-1}, \mathcal{T})},$$

provided that $d(\mathbf{a}_{i,t-1}, \mathcal{T}) > 0$. In other words, the rate of progress $\lambda_{i,t}$ of individual i between time $t-1$ and t reveals how much the distance between individual i 's position and the target's position \mathcal{T} is reduced between time $t-1$ and t .

2.2.2. *Special case 1: Euclidean space.* In the special case $\mathbb{M} := \mathbb{R}^q$ ($q \geq 1$) and $d(\mathbf{a}_{i,t}, \mathcal{T}) := \|\mathbf{a}_{i,t} - \mathcal{T}\|_2$, it is convenient to choose G and H to be multivariate Gaussians. A demonstration of the process model in the special case $\mathbb{M} := \mathbb{R}^2$ and $d(\mathbf{a}_{i,t}, \mathcal{T}) := \|\mathbf{a}_{i,t} - \mathcal{T}\|_2$ is provided by Figure 2.

2.2.3. *Special case 2: hyperbolic space.* An alternative to Euclidean space is a space with an intrinsic hierarchical structure, such as hyperbolic space. For example, consider the two-dimensional Poincaré disk with radius $\rho \in (0, +\infty)$, that is, $\mathbb{M} := \{\mathbf{x} \in \mathbb{R}^2 : \|\mathbf{x}\|_2 < \rho\}$. The distance between the position $\mathbf{a}_{i,t} \in \mathbb{M}$ of individual i at time t and target $\mathcal{T} \in \mathbb{M}$ on the Poincaré disk with radius ρ is defined by

$$d(\mathbf{a}_{i,t}, \mathcal{T}) := \operatorname{arcosh} \left(1 + \frac{2 \rho^2 \|\mathbf{a}_{i,t} - \mathcal{T}\|_2^2}{(\rho^2 - \|\mathbf{a}_{i,t}\|_2^2) (\rho^2 - \|\mathcal{T}\|_2^2)} \right).$$

It is then convenient to choose G and H to be the Uniform distribution on $\{\mathbf{x} \in \mathbb{R}^2 : \|\mathbf{x}\|_2 < \rho\}$.

2.3. *Selecting the geometry of the metric space.* An open issue is how to select the geometry of the metric space (\mathbb{M}, d) . In the statistical analysis of network data, recent work by [Lubold et al. \(2023\)](#) introduced a promising approach to selecting the geometry of latent space models of network data, although the approach of [Lubold et al. \(2023\)](#) falls outside of the Bayesian framework considered here. That said, we expect that the pioneering work of [Lubold et al. \(2023\)](#) paves the way for Bayesian approaches to selecting the geometry of the underlying space, for models of network data and models of educational data. In the special case $\mathbb{M} := \mathbb{R}^q$, an additional issue may arise, in that the dimension q of \mathbb{R}^q may be unknown. Since we are interested in dimension reduction (embedding both individuals and variables in a low-dimensional space) and helping professionals (e.g., educators, medical professionals) assess the progress of individuals by using an easy-to-interpret interaction map, it is tempting to choose a low-dimensional Euclidean space, e.g., \mathbb{R}^2 or \mathbb{R}^3 . In the simulations and applications in Sections 4, 5, and 6, we compare metric spaces (\mathbb{M}, d) with $\mathbb{M} := \mathbb{R}^q$ and $q \in \{1, 2, 3, 4\}$ by using the Watanabe–Akaike information criterion ([Watanabe, 2013](#)) along with interaction maps in \mathbb{R} , \mathbb{R}^2 , and \mathbb{R}^3 .

2.4. *Comparison with existing approaches.* A classic approach to measuring progress of students in educational assessments is based on [Andersen’s \(1985\)](#) model. [Andersen’s \(1985\)](#) model assumes that binary responses $Y_{i,j,t} \in \{0, 1\}$ are independent Bernoulli($\mu_{i,j,t}$) random variables with $\text{logit}(\mu_{i,j,t}) := \alpha_{i,t} + \beta_j$.

To compare [Andersen’s \(1985\)](#) model with the proposed latent process model, consider binary responses $Y_{i,j,t} \in \{0, 1\}$ by students i to items j at $T = 2$ time points $t \in \{1, 2\}$ along with the following reparameterization of [Andersen’s \(1985\)](#) model:

$$\begin{aligned}\alpha_{i,1} &:= -\gamma d(\mathbf{a}_{i,1}, \mathcal{T}) \\ \alpha_{i,2} &:= -\gamma d(\mathbf{a}_{i,2}, \mathcal{T}) = -\gamma(1 - \lambda_{i,2}) d(\mathbf{a}_{i,1}, \mathcal{T}) = (1 - \lambda_{i,2}) \alpha_{i,1},\end{aligned}$$

where $\gamma \in [0, +\infty)$ and $d(\mathbf{a}_{i,t}, \mathcal{T}) := \|\mathbf{a}_{i,t} - \mathcal{T}\|_2$ ($t \in \{1, 2\}$). Then the rate of progress $\lambda_{i,2}$ of student i between time 1 and 2 is a function of the distances $d(\mathbf{a}_{i,1}, \mathcal{T})$ and $d(\mathbf{a}_{i,2}, \mathcal{T})$:

$$\lambda_{i,2} = 1 - \frac{\alpha_{i,2}}{\alpha_{i,1}} = 1 - \frac{d(\mathbf{a}_{i,2}, \mathcal{T})}{d(\mathbf{a}_{i,1}, \mathcal{T})},$$

provided that $d(\mathbf{a}_{i,1}, \mathcal{T}) > 0$. In other words, the higher the ability $\alpha_{i,2}$ of student i at time 2 relative to the ability $\alpha_{i,1}$ of student i at time 1 is, the higher is the rate of progress $\lambda_{i,2}$ of student i between time 1 and 2.

While it may be comforting to know that the abilities $\alpha_{i,1}$ and $\alpha_{i,2}$ of student i at time 1 and 2 can be interpreted in terms of distances $d(\mathbf{a}_{i,1}, \mathcal{T})$ and $d(\mathbf{a}_{i,2}, \mathcal{T})$ between student i and learning target \mathcal{T} in an underlying metric space (\mathbb{M}, d) and that $1 - \alpha_{i,2}/\alpha_{i,1}$ can be interpreted as the rate of progress of student i towards learning target \mathcal{T} , [Andersen’s \(1985\)](#) model has multiple drawbacks:

1. [Andersen’s \(1985\)](#) model assumes that

$$\text{logit}(\mu_{i,j,t}) := \alpha_{i,t} + \beta_j$$

is additive in the ability $\alpha_{i,t}$ of student i at time t and the easiness β_j of item j and therefore cannot capture interactions between students i and items j arising from unobserved variables,

such as cultural background, upbringing, and mentoring. As a result, the underlying metric space (\mathbb{M}, d) of Andersen's (1985) reparameterized model cannot be interpreted as an interaction map, but should be interpreted as an ability map: In fact, the distances $d(\mathbf{a}_{i,1}, \mathcal{T}) \propto \alpha_{i,1}$ and $d(\mathbf{a}_{i,2}, \mathcal{T}) \propto \alpha_{i,2}$ of individual i to target \mathcal{T} at time 1 and 2 are proportional to the abilities $\alpha_{i,1}$ and $\alpha_{i,2}$. By contrast, the proposed latent process model assumes that

$$\text{logit}(\mu_{i,j,t}) := \begin{cases} \alpha_i + \beta_j - \gamma d(\mathbf{a}_{i,1}, \mathbf{b}_j) & \text{if } t = 1 \\ \alpha_i + \beta_j - \gamma (1 - \lambda_{i,2}) d(\mathbf{a}_{i,1}, \mathcal{T}) & \text{if } t = 2 \end{cases}$$

and can hence capture interactions between individuals (e.g., students) and variables (e.g., items): e.g., in educational assessments, a large distance between student i and item j indicates that the probability of a correct response of student i to item j is lower than would be expected based on the ability α_i of student i and the easiness β_j of item j . As a consequence, the underlying metric space (\mathbb{M}, d) of the proposed latent process model should be interpreted as an interaction map rather than an ability map.

2. The fact that the metric space (\mathbb{M}, d) underlying Andersen's (1985) reparameterized model represents an ability map gives rise to an additional limitation of Andersen's (1985) model: If, e.g., $\mathbb{M} := \mathbb{R}^q$ ($q \geq 1$) and $d(\mathbf{a}_{i,t}, \mathcal{T}) := \|\mathbf{a}_{i,t} - \mathcal{T}\|_2$, then $q = 1$ dimension is sufficient for representing the distances $d(\mathbf{a}_{i,t}, \mathcal{T})$ between individuals i at time t and learning target \mathcal{T} in (\mathbb{M}, d) . A Euclidean space \mathbb{R}^q of dimension $q \geq 2$ would provide a less parsimonious representation than $q = 1$ and therefore $q = 1$ is preferable to $q \geq 2$ according to Occam's razor (Jeffreys and Berger, 1992). By contrast, the metric space (\mathbb{M}, d) underlying the proposed latent process model represents an interaction map rather than an ability map. To capture interactions between individuals and variables, a Euclidean space \mathbb{R}^q of dimension $q \geq 2$ may be required. The applications in Sections 5 and 6 demonstrate that.
3. Andersen's (1985) reparameterized model does not separate the abilities $\alpha_{i,1}$ and $\alpha_{i,2}$ of individual i at time 1 and 2 from the rate of progress $\lambda_{i,2}$ of individual i between time 1 and 2, but assumes that the rate of progress $\lambda_{i,2} = 1 - \alpha_{i,2} / \alpha_{i,1}$ is a function of the abilities $\alpha_{i,1}$ and $\alpha_{i,2}$. By contrast, the proposed latent process model separates the ability α_i of individual i from the rate of progress $\lambda_{i,2}$ of individual i between time 1 and 2.
4. The classic approach to assessing progress based on Andersen's (1985) model and its extensions helps estimate how much progress individuals i make (model estimation), but does not determine whether individuals i make progress (model selection). By contrast, the proposed latent process model does double duty: It helps determine whether individuals i make progress (model selection), in addition to estimating how much progress individuals i make (model estimation), and how much more progress individuals i can make in the future.

2.5. *Other possible approaches to measuring progress.* There are other possible approaches to measuring progress, both within and outside of the proposed statistical framework.

To demonstrate, recall that the proposed statistical framework builds on generalized linear models. In other words, the responses $Y_{i,j,t}$ have exponential-family distributions $\mathbb{P}_{\theta, \mathbf{a}_{i,t}, \mathbf{b}_j}$ (Sundberg, 2019; Efron, 2022). In the language of exponential families, the proposed statistical framework measures progress based on the canonical parameterization of the exponential family. An alternative would be to measure progress based on the mean-value parameterization of the exponential family.

To compare these alternative approaches to assessing progress, let $\mathbf{Y}_i := (Y_{i,j,t})_{1 \leq j \leq p, 1 \leq t \leq T}$ be the vector of responses $Y_{i,j,t}$ of individual i and let the distributions $\mathbb{P}_{\boldsymbol{\theta}, \mathbf{a}_{i,t}, \mathbf{b}_j}$ of responses $Y_{i,j,t}$ be one-parameter exponential-family distributions (e.g., $Y_{i,j,t} \mid \mu_{i,j,t} \stackrel{\text{ind}}{\sim} \text{Bernoulli}(\mu_{i,j,t})$ with mean $\mu_{i,j,t} \in (0, 1)$, $Y_{i,j,t} \mid \mu_{i,j,t} \stackrel{\text{ind}}{\sim} \text{Poisson}(\mu_{i,j,t})$ with mean $\mu_{i,j,t} \in (0, +\infty)$, or $Y_{i,j,t} \mid \mu_{i,j,t}, \sigma_{i,j,t}^2 \stackrel{\text{ind}}{\sim} N(\mu_{i,j,t}, \sigma_{i,j,t}^2)$ with mean $\mu_{i,j,t} \in \mathbb{R}$ and known variance $\sigma_{i,j,t}^2 \in (0, +\infty)$). Then the probability density function of an exponential-family probability measure $\mathbb{P}_{\boldsymbol{\theta}, \mathbf{a}_{i,t}, \mathbf{b}_j}$ dominated by a σ -finite measure ν can be represented as

$$f(y_{i,j,t} \mid \eta_{i,j,t}) = a_{i,j,t}(y_{i,j,t}) \exp(\eta_{i,j,t} s_{i,j,t}(y_{i,j,t}) - \psi_{i,j,t}(\eta_{i,j,t})),$$

where $a_{i,j,t}(y_{i,j,t}) \in [0, +\infty)$ is a function of $y_{i,j,t}$, $\eta_{i,j,t} \equiv \eta_{i,j,t}(\mu_{i,j,t}(\boldsymbol{\theta}, \mathbf{a}_{i,t}, \mathbf{b}_j)) \in \mathbb{R}$ is a canonical parameter, $s_{i,j,t}(y_{i,j,t}) \in \mathbb{R}$ is a sufficient statistic, and

$$\psi_{i,j,t}(\eta_{i,j,t}) := \int_{\mathcal{Y}_{i,j,t}} \exp(\eta_{i,j,t} s_{i,j,t}(y_{i,j,t})) d\nu(y_{i,j,t})$$

ensures that $f(y_{i,j,t} \mid \eta_{i,j,t})$ integrates to 1; note that the general formulation above covers both the discrete setting (in which case ν may be counting measure) and the continuous setting (in which case ν may be Lebesgue measure). As a result, the probability density function of the response vector \mathbf{Y}_i of individual i can be represented as

$$f(\mathbf{y}_i \mid \boldsymbol{\eta}_i) = \prod_{j=1}^p \prod_{t=1}^T f(y_{i,j,t} \mid \eta_{i,j,t}) = a_i(\mathbf{y}_i) \exp(\langle \boldsymbol{\eta}_i, \mathbf{s}_i(\mathbf{y}_i) \rangle - \psi_i(\boldsymbol{\eta}_i)),$$

where $a_i(\mathbf{y}_i) := \prod_{j=1}^p \prod_{t=1}^T a_{i,j,t}(y_{i,j,t})$, $\psi_i(\boldsymbol{\eta}_i) := \sum_{j=1}^p \sum_{t=1}^T \psi_{i,j,t}(\eta_{i,j,t})$, and $\langle \boldsymbol{\eta}_i, \mathbf{s}_i(\mathbf{y}_i) \rangle$ denotes the inner product of the vector of canonical parameters $\boldsymbol{\eta}_i := (\eta_{i,j,t})_{1 \leq j \leq p, 1 \leq t \leq T}$ and the vector of sufficient statistics $\mathbf{s}_i(\mathbf{y}_i) := (s_{i,j,t}(y_{i,j,t}))_{1 \leq j \leq p, 1 \leq t \leq T}$. In other words, if the responses $Y_{i,j,t}$ have exponential-family distributions, so does the response vector \mathbf{Y}_i of individual i . The parameter vector

$$\boldsymbol{\mu}_i(\boldsymbol{\eta}_i) := \mathbb{E}_{\boldsymbol{\eta}_i} \mathbf{s}_i(\mathbf{Y}_i)$$

with coordinates $\mu_{i,j,t}(\boldsymbol{\eta}_i) := \mathbb{E}_{\boldsymbol{\eta}_i} s_{i,j,t}(Y_{i,j,t})$ is known as the mean-value parameter vector of the exponential family. Since the map $\boldsymbol{\eta}_i \mapsto \boldsymbol{\mu}_i(\boldsymbol{\eta}_i)$ is a homeomorphism and is hence one-to-one (Brown, 1986, Theorem 3.6, p. 74), one can parameterize the model by using either the canonical parameter vector $\boldsymbol{\eta}_i$ or the mean-value parameter vector $\boldsymbol{\mu}_i(\boldsymbol{\eta}_i)$. As a consequence, one can measure progress based on either the canonical parameterization or the mean-value parameterization: e.g., if the responses $Y_{i,j,t}$ of individual i to variables j have been recorded at $T = 2$ time points, one could measure progress based on differences in mean-value parameters $\mu_{i,j,2}(\boldsymbol{\eta}_i)$ and $\mu_{i,j,1}(\boldsymbol{\eta}_i)$, summed over all variables j :

$$\text{progress of individual } i := \sum_{j=1}^p [\mu_{i,j,2}(\boldsymbol{\eta}_i) - \mu_{i,j,1}(\boldsymbol{\eta}_i)].$$

In addition, one could assess how much more progress individual i can make in the future:

$$\text{possible progress of individual } i \text{ in the future} := \sum_{j=1}^p \left[\sup_{\boldsymbol{\eta}_i} \mu_{i,j,2}(\boldsymbol{\eta}_i) - \mu_{i,j,2}(\boldsymbol{\eta}_i) \right].$$

That being said, the mean-value parameterization is less convenient for the purpose of model selection, e.g., the problem of determining whether students make progress. In fact, it is common practice to base model selection of generalized linear models on the canonical parameterization rather than the mean-value parameterization of exponential families. Therefore, we assess whether and how much progress individuals i make towards the target of interest \mathcal{T} based on the canonical parameterization rather than the mean-value parameterization. The resulting statistical framework comes with the benefit of model selection (e.g., determining whether individuals make progress) and inherits the advantages of the [Jeon et al. \(2021\)](#) model, which is likewise based on the canonical parameterization rather than the mean-value parameterization.

2.6. Priors. We assume that $\alpha_i \mid \mu_\alpha, \sigma_\alpha^2 \stackrel{\text{iid}}{\sim} N(\mu_\alpha, \sigma_\alpha^2)$, $\beta_j \mid \mu_\beta, \sigma_\beta^2 \stackrel{\text{iid}}{\sim} N(\mu_\beta, \sigma_\beta^2)$, and $\gamma \mid \sigma_\gamma^2 \sim \text{Half-Normal}(0, \sigma_\gamma^2)$. The hyperparameters $\mu_\alpha \in \mathbb{R}$ and $\mu_\beta \in \mathbb{R}$ are set to 0 to address identifiability issues (see Section 2.7), while hyperparameter $\sigma_\alpha^2 \in (0, +\infty)$ is assigned hyperprior $\sigma_\alpha^2 \mid a_{\sigma_\alpha}, b_{\sigma_\alpha} \sim \text{Inverse-Gamma}(a_{\sigma_\alpha}, b_{\sigma_\alpha})$. The hyperparameters $\sigma_\beta^2 \in (0, +\infty)$, $\sigma_\gamma^2 \in (0, +\infty)$, $a_{\sigma_\alpha} \in (0, +\infty)$ and $b_{\sigma_\alpha} \in (0, +\infty)$ need to be specified by users. A flexible prior of $\lambda_{i,t}$ can be specified by

$$\text{logit}(\lambda_{i,t}) \mid \pi_{i,t}, \mu_0, \sigma_0^2, \mu_1, \sigma_1^2 \stackrel{\text{ind}}{\sim} (1 - \pi_{i,t}) N(\mu_0, \sigma_0^2) + \pi_{i,t} N(\mu_1, \sigma_1^2),$$

where $\pi_{i,t} \in (0, 1)$. The hyperparameters $(\mu_0, \sigma_0^2) \in \mathbb{R} \times (0, +\infty)$ and $(\mu_1, \sigma_1^2) \in \mathbb{R} \times (0, +\infty)$ are chosen so that the distribution of $\lambda_{i,t}$ is a mixture of two distributions, one of them placing 95% of its mass between .01 and .21 and the other placing 95% of its mass between .04 and .96. The resulting two-component mixture prior of $\lambda_{i,t}$ is motivated by the observation that often some individuals make negligible progress while others make non-negligible progress. The two-component mixture prior of $\lambda_{i,t}$ is shown in Figure 3. The mixing proportions $\pi_{i,t}$ have priors $\pi_{i,t} \mid a_\pi, b_\pi \stackrel{\text{iid}}{\sim} \text{Beta}(a_\pi, b_\pi)$, with hyperparameters $a_\pi \in (0, +\infty)$ and $b_\pi \in (0, +\infty)$.

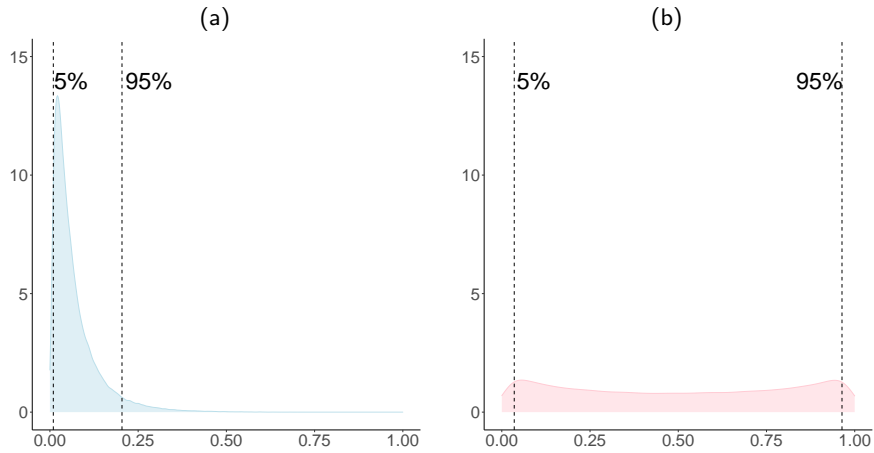


FIG 3. The two component distributions of the two-component mixture prior for the rates of progress $\lambda_{i,t}$, with 5% and 95% percentiles indicated by dashed vertical lines.

2.7. *Identifiability issues.* A well-known issue of the classic Rasch (1960) model and its extensions (including the proposed latent process model) is that the weights α_i and β_j cannot be all estimated, unless additional restrictions are imposed. We follow Gelman and Hill (2007, p. 316) by impose the constraints $\mu_\alpha := 0$ and $\mu_\beta := 0$.

In the special case $\mathbb{M} := \mathbb{R}^2$ and $d(\mathbf{a}_{i,t}, \mathcal{T}) := \|\mathbf{a}_{i,t} - \mathcal{T}\|_2$, the latent process model has the same identifiability issues as other Euclidean latent space models (e.g., Hoff et al., 2002), in that the distances $d(\mathbf{a}_{i,t}, \mathcal{T})$ are invariant to reflection, translation, and rotation of the positions $\mathbf{a}_{i,t}$ of individuals i at time t and target \mathcal{T} . Such identifiability issues can be addressed by Procrustes matching (Hoff et al., 2002).

An additional identifiability issue arises from the fact that, for all $c \in (0, 1) \cup (1, +\infty)$,

$$\eta_{i,j,t}(\mu_{i,j,t}(\boldsymbol{\theta}, \mathbf{a}_{i,t}, \mathbf{b}_j)) := \alpha_i + \beta_j - \gamma \|\mathbf{a}_{i,t} - \mathcal{T}\|_2 = \alpha_i + \beta_j - \frac{\gamma}{c} \|c\mathbf{a}_{i,t} - c\mathcal{T}\|_2,$$

where $\mathcal{T} := (1/p) \sum_{j=1}^p \mathbf{b}_j$. Such identifiability issues can be addressed by constraining either the positions $\mathbf{a}_{i,t}$ of individuals i at time t or the positions \mathbf{b}_j of variables j (but not both). We constrain the positions \mathbf{b}_j of variables j , adapting the constraint of Handcock et al. (2007):

$$\sqrt{\frac{1}{p} \sum_{j=1}^p \|\mathbf{b}_j\|_2^2} = 1.$$

We do not constrain the positions $\mathbf{a}_{i,t}$ of individuals i at time t .

3. Bayesian inference. Define $\mathbf{y} := (y_{i,j,t})_{1 \leq i \leq n, 1 \leq j \leq p, 1 \leq t \leq T}$, $\boldsymbol{\alpha} := (\alpha_i)_{1 \leq i \leq n}$, $\boldsymbol{\beta} := (\beta_j)_{1 \leq j \leq p}$, $\boldsymbol{\lambda} := (\lambda_{i,t})_{1 \leq i \leq n, 2 \leq t \leq T}$, $\boldsymbol{\pi} := (\pi_{i,t})_{1 \leq i \leq n, 2 \leq t \leq T}$, $\mathbf{A} := (\mathbf{a}_{i,t})_{1 \leq i \leq n, 1 \leq t \leq T}$, and $\mathbf{B} := (\mathbf{b}_j)_{1 \leq j \leq p}$. Then the posterior is proportional to

$$\begin{aligned} f(\boldsymbol{\alpha}, \boldsymbol{\beta}, \gamma, \mathbf{A}, \mathbf{B}, \boldsymbol{\lambda}, \boldsymbol{\pi} \mid \mathbf{y}) &\propto \left[\prod_{i=1}^n \prod_{j=1}^p \prod_{t=1}^T f(y_{i,j,t} \mid \alpha_i, \beta_j, \gamma, \mathbf{a}_{i,t}, \mathbf{b}_1, \dots, \mathbf{b}_p) \right] \\ &\times \left[\prod_{i=1}^n f(\alpha_i \mid \sigma_\alpha^2) \right] \times f(\sigma_\alpha^2) \times \left[\prod_{j=1}^p f(\beta_j) \right] \times f(\gamma) \\ &\times \left[\prod_{i=1}^n f(\mathbf{a}_{i,1}) \prod_{t=2}^T f(\mathbf{a}_{i,t} \mid \mathbf{a}_{i,t-1}, \mathbf{b}_1, \dots, \mathbf{b}_p, \lambda_{i,t}) \right] \\ &\times \left[\prod_{j=1}^p f(\mathbf{b}_j) \right] \times \left[\prod_{i=1}^n \prod_{t=2}^T f(\lambda_{i,t} \mid \pi_{i,t}) f(\pi_{i,t}) \right]. \end{aligned}$$

Here, in an abuse of notation, f denotes a probability mass or density function with suitable support. It is worth noting that the conditional densities $f(\mathbf{a}_{i,t} \mid \mathbf{a}_{i,t-1}, \mathbf{b}_1, \dots, \mathbf{b}_p, \lambda_{i,t})$ are point masses, because the positions $\mathbf{a}_{i,t} := (1 - \lambda_{i,t}) \mathbf{a}_{i,t-1} + \lambda_{i,t} \mathcal{T}$ of individuals i at time t are non-random functions of $\mathbf{a}_{i,t-1}$, $\mathcal{T} := (1/p) \sum_{j=1}^p \mathbf{b}_j$, and $\lambda_{i,t}$ for fixed $\mathbf{a}_{i,t-1}$, $\mathbf{b}_1, \dots, \mathbf{b}_p$, and $\lambda_{i,t}$.

We approximate the posterior by Markov chain Monte Carlo: e.g., if all responses $Y_{i,j,t} \in \{0, 1\}$ are binary, we use the Pólya-Gamma sampler of [Polson et al. \(2013\)](#) for updating unknown quantities in the data model and Gibbs samplers and Metropolis-Hasting steps for updating unknown quantities in the process model. Details are provided in Supplement B.

4. Simulations. We investigate whether the proposed statistical framework can capture interesting features of real-world data that have not been generated by the model. In other words, we investigate the behavior of the proposed statistical framework under model misspecification.

Throughout Sections 4, 5, and 6, we focus on binary responses $Y_{i,j,t} \in \{0, 1\}$ at $T = 2$ time points $t \in \{1, 2\}$ and write λ_i instead of $\lambda_{i,2}$. All results are based on the proposed latent process model with a logit link function and the special case $\mathbb{M} := \mathbb{R}^q$ and $d(\mathbf{a}_{i,t}, \mathcal{T}) := \|\mathbf{a}_{i,t} - \mathcal{T}\|_2$. We compare results based on $\mathbb{M} := \mathbb{R}, \mathbb{R}^2, \mathbb{R}^3$, and \mathbb{R}^4 using the Watanabe–Akaike information criterion ([Watanabe, 2013](#)) along with interaction maps based on \mathbb{R}, \mathbb{R}^2 , and \mathbb{R}^3 . The prior and Markov chain Monte Carlo algorithm are described in Supplement C.

\mathbb{M}	10% Percentile	Median	90% Percentile	Minimizer of WAIC
$\mathbb{M} := \mathbb{R}$	17937	18170	19228	2.0%
$\mathbb{M} := \mathbb{R}^2$	17639	17815	18016	73.2%
$\mathbb{M} := \mathbb{R}^3$	17613	18129	18391	21.6%
$\mathbb{M} := \mathbb{R}^4$	18075	18304	18512	3.2%

TABLE 1

Simulation results ($n = 300$): Watanabe–Akaike information criterion (WAIC) based on 250 simulated data sets. The last column indicates how often the latent process model with $\mathbb{M} := \mathbb{R}, \mathbb{R}^2, \mathbb{R}^3, \mathbb{R}^4$ minimized the WAIC.

4.1. *Scenario $n = 300, p = 10, T = 2$.* We first consider a scenario in which the progress of individuals towards a target of interest $\mathcal{T} \in \mathbb{M} := \mathbb{R}^q$ is assessed based on binary responses $Y_{i,j,t} \in \{0, 1\}$ of $n = 300$ individuals to $p = 10$ variables at $T = 2$ time points $t \in \{1, 2\}$. We assume that there are three groups of individuals, called G1, G2, and G3. Each group is comprised of 100 individuals. At time 1, the success probabilities of all individuals are .2. At time 2, individuals have success probabilities .25 (G1), .5 (G2), and .75 (G3). We generated 250 data sets and estimated the latent process model with $\mathbb{M} := \mathbb{R}^q$ and $q \in \{1, 2, 3, 4\}$.

The Watanabe–Akaike information criterion ([Watanabe, 2013](#)) in Table 1 suggests that the latent process model with $\mathbb{M} := \mathbb{R}^2$ is more adequate than $\mathbb{M} := \mathbb{R}, \mathbb{R}^3$, and \mathbb{R}^4 .

A natural question to ask is whether the latent process model can separate groups G1, G2, and G3 based on data. Figure 4 indicates that the latent process model with $\mathbb{M} := \mathbb{R}^q$ and $q \in \{1, 2, 3\}$ can distinguish groups G1, G2, and G3, despite the fact that the data were not generated by the model. That said, the latent process model with $\mathbb{M} := \mathbb{R}^2$ or \mathbb{R}^3 can better distinguish groups G1, G2, and G3 than the latent process model with $\mathbb{M} := \mathbb{R}$, reinforcing the findings in Table 1.

A related question is whether the latent process model can distinguish individuals with non-negligible progress from those with negligible progress, based on the two-component mixture prior for the rates of progress λ_i of individuals i described in Section 2.6. Figure 5 reveals that—among the 100 individuals in groups G1, G2, and G3—the percentage of individuals deemed to have made negligible progress is more than 80% in the low-progress group G1; is between 40% and 80% in the moderate-progress group G2; and is less than 20% in the high-progress group G3. The latent

process model with $\mathbb{M} := \mathbb{R}^2$ or \mathbb{R}^3 seems to lead to more accurate assessments, compared with the latent process model with $\mathbb{M} := \mathbb{R}$.

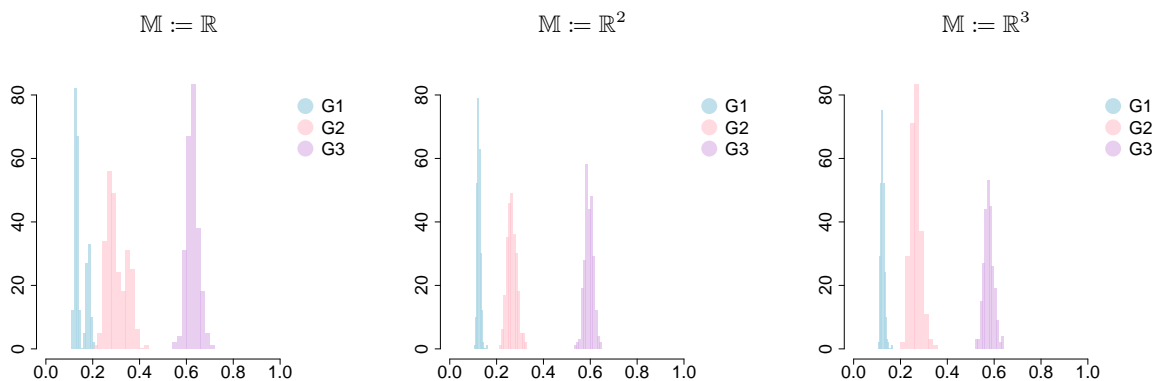


FIG 4. Simulation results ($n = 300$): Histogram of the posterior medians of the rates of progress λ_i of individuals i in groups $G1$, $G2$, $G3$.

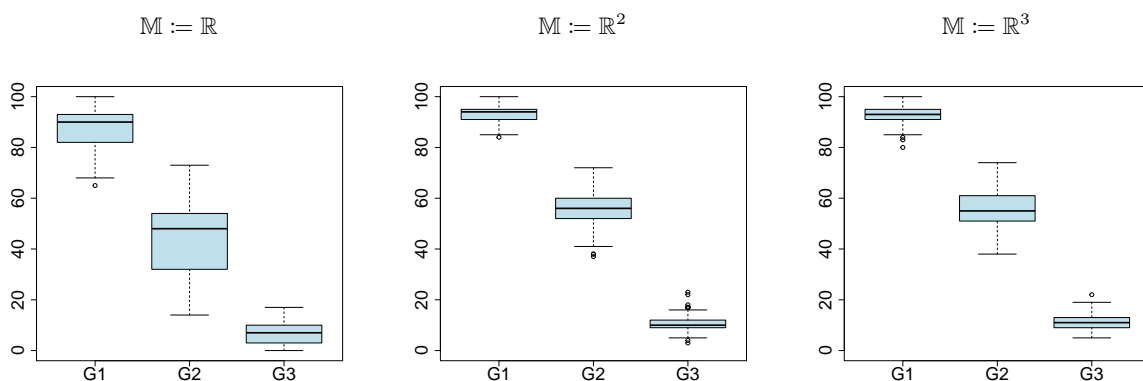


FIG 5. Simulation results ($n = 300$): Boxplots of the number of individuals in groups $G1$, $G2$, $G3$ deemed to have made negligible progress.

4.2. *Scenario $n = 600$, $p = 10$, $T = 2$.* We double the sample size from $n = 300$ to $n = 600$ to explore the behavior of the latent process model as the sample size increases. We assume that there are four groups of individuals, called $G1$, $G2$, $G3$ and $G4$. Each group is comprised of 150 individuals. At time 1 the success probabilities of all individuals are .2, while at time 2 individuals have success probabilities .3 ($G1$), .5 ($G2$), .7 ($G3$), and .9 ($G4$). We generated 250 data sets and estimated the latent process model with $\mathbb{M} := \mathbb{R}^q$ and $q \in \{1, 2, 3, 4\}$.

The results dovetail with the results in Section 4.1, but suggest that the one-dimensional space $\mathbb{M} := \mathbb{R}$ is even less appealing when n is large: First, the Watanabe–Akaike information criterion (Watanabe, 2013) in Table 2 favors $\mathbb{M} := \mathbb{R}^2$ over \mathbb{R} , \mathbb{R}^3 , and \mathbb{R}^4 . Second, the latent process model can distinguish the groups $G1$, $G2$, $G3$, and $G4$ when $\mathbb{M} := \mathbb{R}^q$ and $q \geq 2$ according to Figure 6, but

\mathbb{M}	10% Percentile	Median	90% Percentile	Minimizer of WAIC
$\mathbb{M} := \mathbb{R}$	35703	36567	38665	10.0%
$\mathbb{M} := \mathbb{R}^2$	35256	35567	35920	79.6%
$\mathbb{M} := \mathbb{R}^3$	35581	36017	36639	10.4%
$\mathbb{M} := \mathbb{R}^4$	36243	36976	38083	0.0%

TABLE 2

Simulation results ($n = 600$): Watanabe–Akaike information criterion (WAIC) based on 250 simulated data sets. The last column indicates how often the latent process model with $\mathbb{M} := \mathbb{R}, \mathbb{R}^2, \mathbb{R}^3, \mathbb{R}^4$ minimized the WAIC.

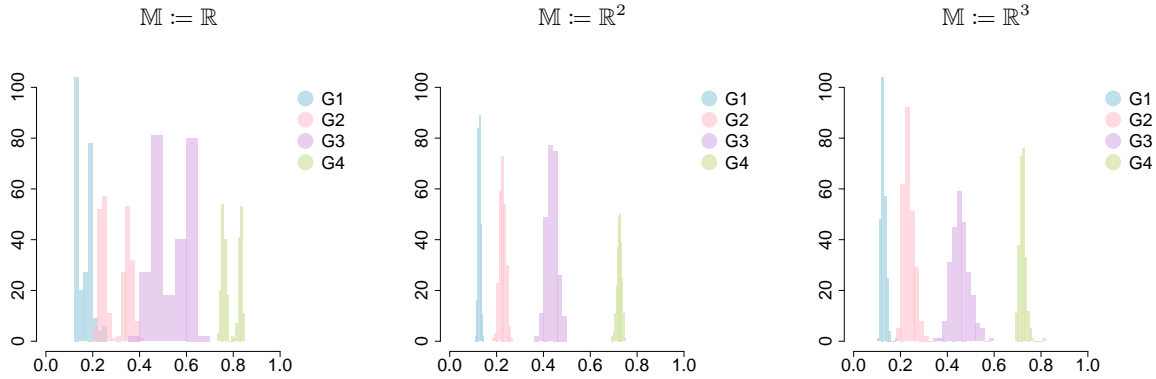


FIG 6. Simulation results ($n = 600$): Histogram of the posterior medians of the rates of progress λ_i of individuals i in groups $G1, G2, G3, G4$.

the groups $G1, G2, G3,$ and $G4$ are less well-separated when $\mathbb{M} := \mathbb{R}$.

5. Application: mental health. We describe the motivating example introduced in Section 1.1 in more detail. The motivating example is concerned with assessing the progress of vulnerable population members in terms of mental health. We focus on a vulnerable population of special interest: mothers with infants in low-income communities.

5.1. *Data.* Santos et al. (2018) conducted between 2003 and 2010 large-scale randomized clinical trials in low-income communities in the U.S. states of North Carolina and New York (Beeber et al., 2014). The data set consists of 306 low-income mothers with infants aged 6 weeks to 36 months, enrolled in the Early Head Start Program in North Carolina or New York. The mental health of these mothers was assessed four times (baseline, 14 weeks, 22 weeks, and 26 weeks). We focus on the $n = 257$ mothers who participated in the first two assessments. The Center for Epidemiological Studies Depression (CES-D) scale was used to measure depression of the mothers. We focus on $p = 10$ items: 1 (“bothered”), 2 (“trouble in concentration”), 3 (“feeling depressed”), 4 (“effort”), 5 (“not feeling hopeful”), 6 (“failure”), 7 (“not happy”), 8 (“talking less”), 9 (“people dislike”), and 10 (“get going”), described in Supplement A. To measure progress toward the target of interest (improving mental health), we recoded the $p = 10$ items by assigning “depression” $\mapsto 0$ and “no depression” $\mapsto 1$. The proportions of positive responses (“no depression”) range from .436 to .747 at the pre-assessment (median .630), and from .621 to .859 at the post-assessment (median .777).

\mathbb{M}	Minimum	Median	Maximum	Minimizer of WAIC
$\mathbb{M} := \mathbb{R}$	14650	14713	14897	0%
$\mathbb{M} := \mathbb{R}^2$	14432	14606	14679	0%
$\mathbb{M} := \mathbb{R}^3$	14351	14450	14509	100%
$\mathbb{M} := \mathbb{R}^4$	14499	14623	14741	0%

TABLE 3

Mental health: Watanabe–Akaike information criterion (WAIC) based on five Markov chain Monte Carlo runs. The last column indicates how often the latent process model with $\mathbb{M} := \mathbb{R}, \mathbb{R}^2, \mathbb{R}^3, \mathbb{R}^4$ minimized the WAIC.

5.2. *Results.* We assess the progress of $n = 257$ low-income mothers towards the target of interest \mathcal{T} (improving mental health), measured by $p = 10$ items. The priors and Markov chain Monte Carlo algorithm can be found in Supplement C. To detect signs of non-convergence, we used trace plots along with the multivariate Gelman–Rubin potential scale reduction factor of Vats and Knudson (2021). These convergence diagnostics are reported in Supplement D and do not reveal signs of non-convergence.

Table 3 shows the Watanabe–Akaike information criterion (Watanabe, 2013) based on the latent process model with $\mathbb{M} := \mathbb{R}^q$ and $q \in \{1, 2, 3, 4\}$, suggesting that $\mathbb{M} := \mathbb{R}^3$ is most appropriate.

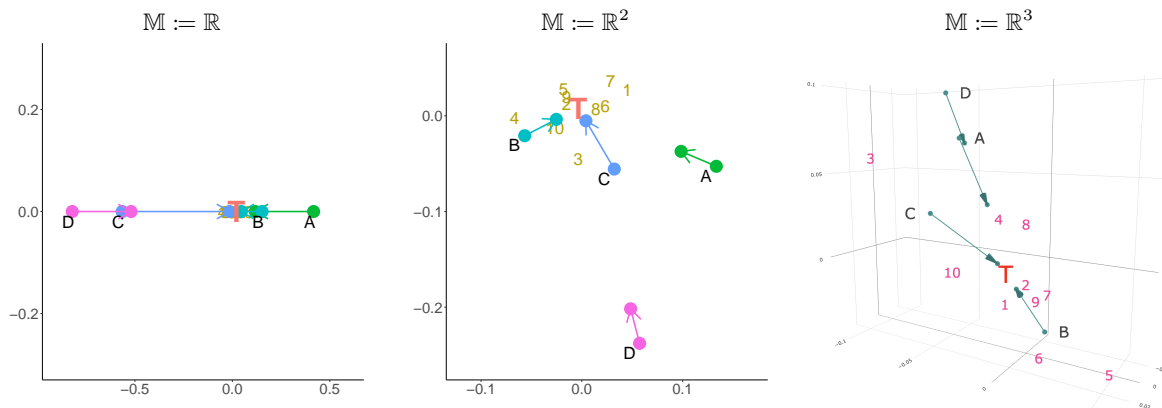


FIG 7. *Mental health: Interaction maps (\mathbb{M}, d) with $\mathbb{M} := \mathbb{R}^q$ and $q \in \{1, 2, 3\}$ show the progress of low-income mothers A, B, C, D towards target \mathcal{T} (improving mental health), measured by items $1, \dots, 10$ (questions about depression). The positions of mothers and items are estimated by posterior medians. While the one-dimensional interaction map ($q = 1$) suggests that all items are close to target \mathcal{T} , the three-dimensional interaction map ($q = 3$) reveals interactions between mothers and items: e.g., item 5 deviates from the bulk of the items, and mother B is closest to item 5. It turns out that mother B agreed with item 5 at the first assessment (“feeling hopeful”), whereas mothers A, C, D did not. In addition, the interaction map suggests that mothers B and C have made strides towards improving mental health, whereas mothers A and D may need to make more progress.*

We present interaction maps in Figure 7. While the one-dimensional interaction map suggests that all items are close to target \mathcal{T} , the three-dimensional interaction map (which, according to the Watanabe–Akaike information criterion, is more appropriate than the one-dimensional interaction map) reveals that there are interactions between individuals (mothers) and items (questions about depression): e.g., item 5 deviates from the bulk of the items, and mother B is closest to item 5. It turns out that mother B agreed with item 5 at the first assessment (“feeling hopeful”), whereas mothers $A, C,$ and D did not. In addition, the interaction map suggests that mothers B and C

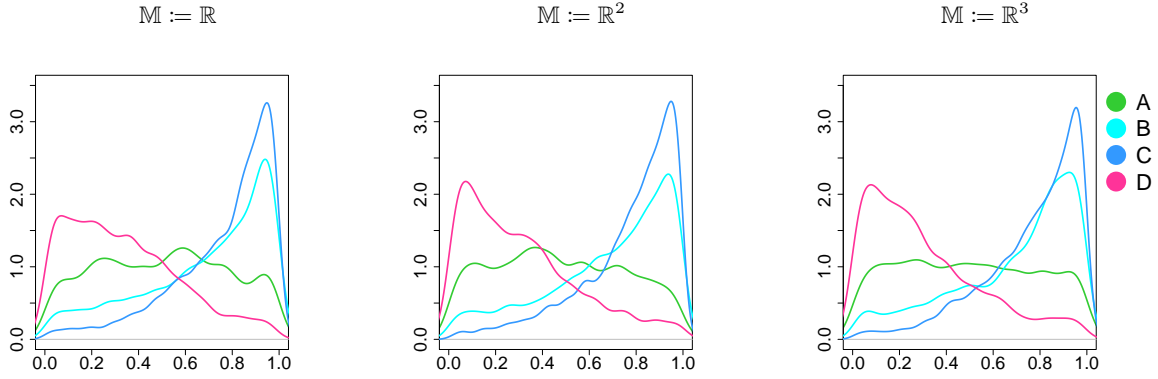


FIG 8. *Mental health: Marginal posteriors of the rates of progress λ_A , λ_B , λ_C , λ_D of mothers A , B , C , D towards target \mathcal{T} (improving mental health). The progress of mother A is unclear, but the marginal posteriors of the rates of progress λ_B and λ_C of mothers B and C have modes close to 1, confirming that mothers B and C have made strides towards improving mental health. By contrast, the mode of the marginal posterior of the rate of progress λ_D of mother D is close to 0, suggesting that mother D may need additional assistance.*

have made strides towards improving mental health, whereas mothers A and D may need to make more progress in the future.

The posterior summaries in Table 4 confirms that, more likely than not, mothers B and C have made progress, while mother D has not. To gain more insight into the uncertainty about the progress of mothers A , B , C , and D , we present the marginal posteriors of λ_A , λ_B , λ_C , and λ_D in Figure 8. The marginal posteriors of λ_A , λ_B , λ_C , and λ_D caution that there is non-negligible uncertainty about the progress of some of the mothers. A case in point is mother A : The marginal posterior of mother A 's rate of progress λ_A resembles the Uniform(0, 1) distribution. As a consequence, it is unclear whether mother A has made progress, and how much. By contrast, the marginal posteriors of the rates of progress λ_B and λ_C of mothers B and C have modes close to 1, suggesting that mothers B and C have made strides towards improving mental health. The marginal posterior of the rate of progress λ_D of mother D has a mode close to 0, which underscores that mother D may need additional assistance.

To assess the goodness-of-fit of the model, we generated 1,000 posterior predictions of the proportions of positive responses at the second assessment. Figure 9 shows the proportions of predicted and observed positive responses. By and large, the model predictions agree with the observations.

6. Application: online educational assessments. We present an application to online educational assessments, using the My Math Academy data (Bang et al., 2022).

6.1. *Data.* The My Math Academy data set consists of 479 kindergarten children, first- and second-grade students who participated in the My Math Academy effectiveness study in 2019 (Bang et al., 2022). The students worked on pre- and post-assessments before and after working on the online learning platform My Math Academy. The pre- and post-assessments were separated by three months, and both included a common set of 31 problems. We focus on $p = 8$ items measuring numerical understanding. Three selected items are presented in Figure 10. We exclude 58 of the 479

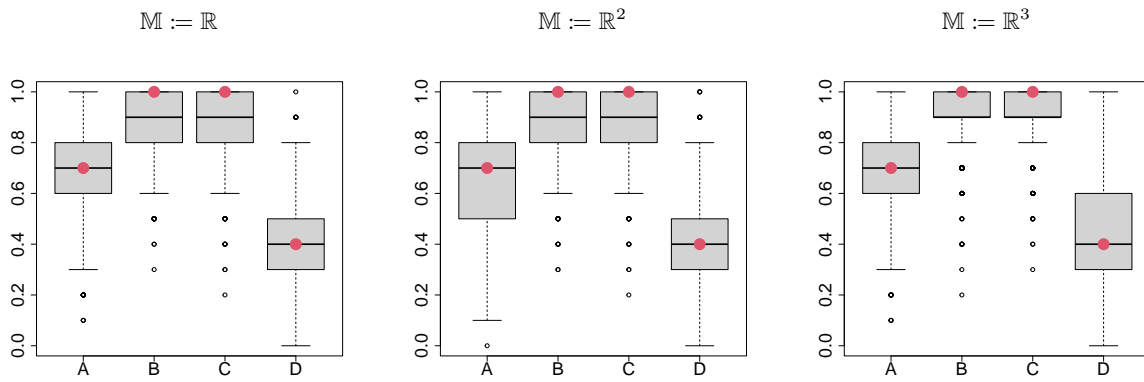


FIG 9. Mental health: Posterior predictions of the proportions of positive responses by mothers A, B, C, D at the second assessment. The observed proportions are indicated by red circles.

Question 24.
Find the missing number.

6 tens + 8 ones = _____

A. 14
B. 86
C. 68

Question 25.
Count the circles, then fill in the missing numbers.

1	2
3	5
4	6

DEST tens + DEST ones = 11

Question 30.
Which number has a seven in the tens place?

A. 7
B. 70
C. 700

FIG 10. My Math Academy: Selected questions 24, 25, 30 corresponding to items 6, 7, 8. Each question has a single correct response. Items 6, 7, 8 are indicators of whether students choose the correct response to questions 24, 25, 30.

	10% Percentile	Median	90% Percentile	Probability: Progress?
$\mathbb{M} := \mathbb{R}$:				
λ_A	.060	.290	.790	.550
λ_B	.085	.578	.950	.707
λ_C	.213	.775	.965	.847
λ_D	.041	.179	.517	.415
$\mathbb{M} := \mathbb{R}^2$:				
λ_A	.055	.255	.757	.518
λ_B	.092	.590	.946	.718
λ_C	.278	.790	.965	.866
λ_D	.039	.147	.463	.377
$\mathbb{M} := \mathbb{R}^3$:				
λ_A	.058	.258	.806	.527
λ_B	.090	.599	.944	.718
λ_C	.280	.774	.969	.861
λ_D	.038	.148	.464	.385

TABLE 4

Mental health: Marginal posteriors of the rates of progress $\lambda_A, \lambda_B, \lambda_C, \lambda_D$ of mothers A, B, C, D. The last column ("Probability: Progress?") shows the posterior probability of non-negligible progress.

children who had no responses at either the pre- or post-assessment or who reported no background information. 55% of the remaining $n = 421$ students are kindergarten children, 48% are female, 87% are low-income students eligible to receive free lunches, 87% are Hispanic, and 6% are African-American. The proportions of correct responses range from .114 to .556 at the pre-assessment (median .397), and from .216 to .755 at the post-assessment (median .544).

\mathbb{M}	Minimum	Median	Maximum	Minimizer of WAIC
$\mathbb{M} := \mathbb{R}$	20209	20310	20597	0%
$\mathbb{M} := \mathbb{R}^2$	19838	20035	20077	60%
$\mathbb{M} := \mathbb{R}^3$	19841	20032	20071	40%
$\mathbb{M} := \mathbb{R}^4$	20166	20436	20678	0%

TABLE 5

My Math Academy: Watanabe–Akaike information criterion (WAIC) based on five Markov chain Monte Carlo runs. The last column indicates how often the latent process model with $\mathbb{M} := \mathbb{R}, \mathbb{R}^2, \mathbb{R}^3, \mathbb{R}^4$ minimized the WAIC.

6.2. *Results.* We assess the progress of $n = 421$ students towards the target of interest (numerical understanding), measured by $p = 8$ items. The prior and Markov chain Monte Carlo algorithm are described in Supplement C. To detect signs of non-convergence, we used trace plots along with the multivariate Gelman-Rubin potential scale reduction factor of Vats and Knudson (2021). These convergence diagnostics can be found in Supplement D and do not reveal signs of non-convergence.

Table 5 shows the Watanabe–Akaike information criterion (Watanabe, 2013) based on the latent process model with $\mathbb{M} := \mathbb{R}^q$ and $q \in \{1, 2, 3, 4\}$. The Watanabe–Akaike information criterion suggests that $\mathbb{M} := \mathbb{R}^2$ or \mathbb{R}^3 is most appropriate.

Figure 11 shows interaction maps, focusing on selected Hispanic students A, B, C, and D in low-income families. While the one-dimensional interaction map suggests that all items are close to learning target \mathcal{J} , the two- and three-dimensional interaction maps (which, according to the Watanabe–Akaike information criterion, are more appropriate than the one-dimensional interaction map) indicate that some of the items deviate from the bulk of the items: e.g., item 6 is the most

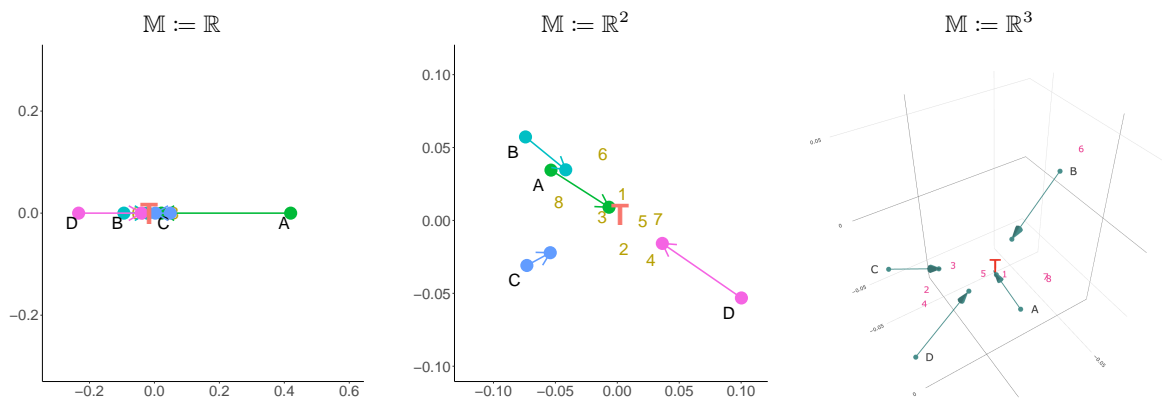


FIG 11. *My Math Academy*: Interaction maps (\mathbb{M}, d) with $\mathbb{M} := \mathbb{R}^q$ and $q \in \{1, 2, 3\}$ show the progress of Hispanic students A, B, C, D in low-income families towards learning target \mathcal{T} (numerical understanding), measured by items $1, \dots, 8$. The positions of students and items are estimated by posterior medians. While the one-dimensional interaction map ($q = 1$) suggests that all items are close to learning target \mathcal{T} , the two- and three-dimensional interaction maps ($q \in \{2, 3\}$) indicate that some of the items deviate from the bulk of the items: e.g., item 6 is the most abstract item among the counting-related items 5, 6, 7 and the two- and three-dimensional interaction map reveal that item 6 deviates from learning target \mathcal{T} more than any other item. Student B is closest to item 6 and provided a correct response to item 6 at the pre-assessment, whereas students A, C, D did not.

abstract item among the counting-related items 5, 6, and 7 and the two- and three-dimensional interaction map reveal that item 6 deviates from learning target \mathcal{T} more than any other item. Student B is closest to item 6 and provided a correct response to item 6 at the pre-assessment, whereas students $A, C,$ and D did not.

Posterior summaries of the rates of progress $\lambda_A, \lambda_B, \lambda_C,$ and λ_D of students $A, B, C,$ and D are shown in Table 6. These posterior summaries confirm that, with high posterior probability, students A and D have made non-negligible progress, but there is more uncertainty about students B and C . To gain more insight into the uncertainty about the progress of students $A, B, C,$ and D , we present the marginal posteriors of the rates of progress $\lambda_A, \lambda_B, \lambda_C,$ and λ_D of students $A, B, C,$ and D in Figure 12. The marginal posteriors reveal non-negligible uncertainty: e.g., the marginal posteriors of the rates of progress λ_A and λ_D of students A and D have modes close to 1, but both of them have long tails. Assessing the progress of students B and C is harder still.

To assess the goodness-of-fit of the model, we generated 1,000 posterior predictions of the proportions of correct responses at the post-assessment. Figure 13 suggests that the posterior predictions by and large match the observed proportions of correct responses.

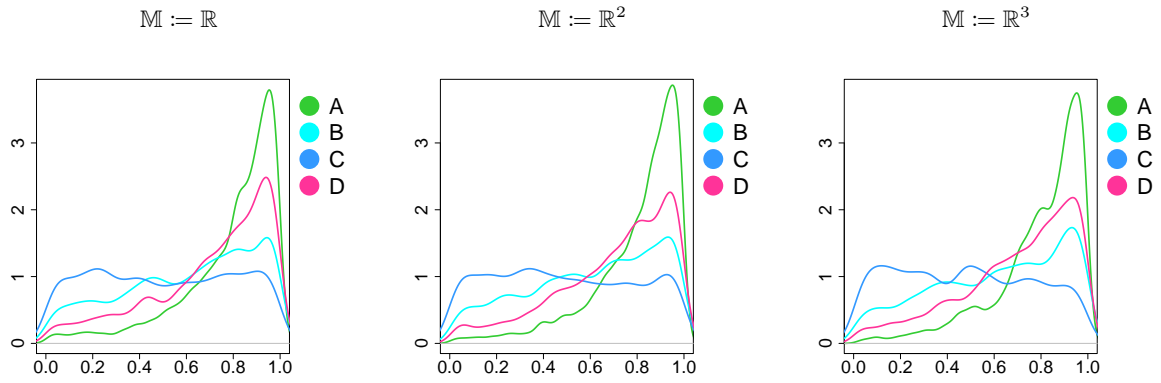


FIG 12. My Math Academy: Marginal posteriors of the rates of progress $\lambda_A, \lambda_B, \lambda_C, \lambda_D$ of Hispanic students A, B, C, D towards learning target \mathcal{T} (numerical understanding).

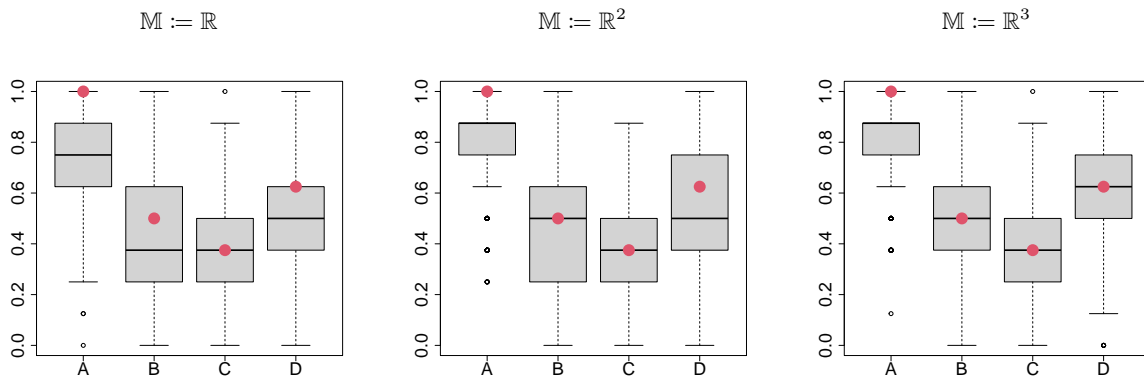


FIG 13. My Math Academy: Posterior predictions of the proportions of correct responses by Hispanic students A, B, C, D at the post-assessment. The observed proportions are indicated by red circles.

	10% Percentile	Median	90% Percentile	Probability: Progress?
$M := \mathbb{R}$:				
λ_A	.196	.817	.970	.863
λ_B	.072	.419	.918	.635
λ_C	.055	.246	.826	.523
λ_D	.107	.648	.953	.743
$M := \mathbb{R}^2$:				
λ_A	.352	.837	.970	.900
λ_B	.080	.424	.913	.642
λ_C	.051	.250	.814	.515
λ_D	.116	.653	.948	.770
$M := \mathbb{R}^3$:				
λ_A	.322	.814	.970	.885
λ_B	.076	.406	.920	.634
λ_C	.051	.227	.771	.498
λ_D	.133	.639	.947	.765

TABLE 6

My Math Academy: Summaries of the marginal posteriors of the rates of progress $\lambda_A, \lambda_B, \lambda_C, \lambda_D$ of students A, B, C, D. The last column ("Probability: Progress?") shows the posterior probability of non-negligible progress.

7. Discussion. We have introduced a latent process model for monitoring progress towards a hard-to-measure target of interest, with a number of possible extensions.

For example, it may be of interest to monitor the progress of individuals towards two or more targets, which may or may not be related. If the targets are known to be unrelated (e.g., improving the command of English language and the understanding of geometry), the targets could be analyzed by separate latent process models, with separate latent spaces. By contrast, if the targets are related (e.g., improving the understanding of random variables and of stochastic processes, i.e., collections of random variables), it may be of interest to monitor the progress of individuals towards both targets. Extensions of the latent process model for tackling multiple targets constitute an interesting direction for future research. A second example is regress, the opposite of progress. Capturing regress is of interest in mental health applications, because the mental health of vulnerable individuals may deteriorate rather than improve.

References.

- Andersen, E. B. (1985), "Estimating latent correlations between repeated testings," *Psychometrika*, 50, 3–16.
- Bang, H., Li, L., and Flynn, K. (2022), "Efficacy of an adaptive game-based math learning app to support personalized learning and improve early elementary school students' learning," *Early Childhood Education Journal*, doi.org/10.1007/s10643-022-01332-3.
- Bansak, C., and Starr, M. (2021), "COVID-19 shocks to education supply: How 200,000 US households dealt with the sudden shift to distance learning," *Review of Economics of the Household*, 19, 63–90.
- Beeber, L., Schwartz, T., Martinez, M., Holditch-Davis, D., Bledsoe, S., and Canuso, R. (2014), "Depressive symptoms and compromised parenting in low-income mothers of infants and toddlers: distal and proximal risks," *Research in Nursing & Health*, 37, 276–291.
- Brown, L. (1986), *Fundamentals of Statistical Exponential Families: With Applications in Statistical Decision Theory*, Hayworth, CA, USA: Institute of Mathematical Statistics.
- Cai, L. (2010), "A two-tier full-information item factor analysis model with applications," *Psychometrika*, 75, 581–612.
- Daly, M., Sutin, A. R., and Robinson, E. (2020), "Longitudinal changes in mental health and the COVID-19 pandemic: evidence from the UK Household Longitudinal Study," *Psychological Medicine*, 1–10.
- Efron, B. (2022), *Exponential Families in Theory and Practice*, Cambridge, MA: Cambridge University Press.
- Embretson, S. E. (1991), "A multidimensional latent trait model for measuring learning and change," *Psychometrika*, 56, 495–515.
- Engzell, P., Frey, A., and Verhagen, M. D. (2021), "Learning loss due to school closures during the COVID-19 pandemic," *Proceedings of the National Academy of Sciences*, 118, e2022376118.
- Gelman, A., and Hill, J. (2007), *Data Analysis Using Regression and Multilevel/Hierarchical Models*, New York: Cambridge University Press.
- Gelman, A., and Rubin, D. (1992), "Inference from iterative simulation using multiple sequences," *Statistical Science*, 7, 457–472.
- Handcock, M. S., Raftery, A. E., and Tantrum, J. M. (2007), "Model-based clustering for social networks," *Journal of the Royal Statistical Society, Series A (with discussion)*, 170, 301–354.
- Hoff, P. D., Raftery, A., and Handcock, M. S. (2002), "Latent space approaches to social network analysis," *Journal of the American Statistical Association*, 97, 1090–1098.
- Holmes, E. A., O'Connor, R. C., Perry, V. H., Tracey, I., Wessely, S., Arseneault, L., and Everall, I. (2020), "Multidisciplinary research priorities for the COVID-19 pandemic: A call for action for mental health science," *The Lancet Psychiatry*, 7, 547–560.
- Huang, H. (2015), "A multilevel higher order item response theory model for measuring latent growth in longitudinal data," *Applied Psychological Measurement*, 39, 362–372.
- Hunter, D. R., Krivitsky, P. N., and Schweinberger, M. (2012), "Computational statistical methods for social network models," *Journal of Computational and Graphical Statistics*, 21, 856–882.
- Jeffreys, W. H., and Berger, J. O. (1992), "Ockham's razor and Bayesian analysis," *American Scientist*, 80, 64–72.
- Jeon, M., Jin, I. H., Schweinberger, M., and Baugh, S. (2021), "Mapping unobserved item-response interactions: A latent space item response model with interaction maps," *Psychometrika*, 86, 378–403.

- Jeon, M., and Rabe-Hesketh, S. (2016), "An autoregressive growth model for longitudinal item analysis," *Psychometrika*, 81, 830–850.
- Krioukov, D., Papadopoulos, F., Kitsak, M., Vahdat, A., and Boguna, M. (2010), "Hyperbolic geometry of complex networks," *Physical Review E*, 82.
- Kuhfeld, M., and et al. (2020), "Projecting the potential impacts of COVID-19 school closures on academic achievement," *Educational Research*, 49, 549–565.
- Lubold, S., Chandrasekhar, A. G., and McCormick, T. H. (2023), "Identifying the latent space geometry of network models through analysis of curvature," *Journal of the Royal Statistical Society: Series B (with discussion)*, 1–63, to appear.
- Pastor, D. A., and Beretvas, S. N. (2006), "Longitudinal Rasch modeling in the context of psychotherapy," *Applied Psychological Measurement*, 30, 100–120.
- Polson, N. G., Scott, J. G., and Windle, J. (2013), "Bayesian inference for logistic models using Pólya–Gamma latent variables," *Journal of the American Statistical Association*, 108, 1339–1349.
- Rasch, G. (1960), *Probabilistic models for some intelligence and attainment tests*, Copenhagen, Denmark: Danish Institute for Educational Research.
- Santos, H. J., Kossakowski, J., Schwartz, T., Beeber, L., and Fried, E. (2018), "Longitudinal network structure of depression symptoms and self-efficacy in low-income mothers," *PLoS ONE*, 13, e0191675.
- Schweinberger, M., and Snijders, T. A. B. (2003), "Settings in social networks: A measurement model," *Sociological Methodology*, 33, 307–341.
- Segawa, E. (2005), "A growth model for multilevel ordinal data," *Journal of Educational and Behavioral Statistics*, 30, 369–396.
- Smith, A. L., Asta, D. M., and Calder, C. A. (2019), "The geometry of continuous latent space models for network data," *Statistical Science*, 34, 428–453.
- Sundberg, R. (2019), *Statistical Modelling by Exponential Families*, Cambridge, UK: Cambridge University Press.
- Tierney, L. (1994), "Markov chains for exploring posterior distributions," *The Annals of Statistics*, 22, 1701–1728.
- Vats, D., and Flegal, J. (2021), "Lugsail lag windows for estimating time-average covariance matrices," *Biometrika*, to appear.
- Vats, D., and Knudson, C. (2021), "Revisiting the Gelman-Rubin Diagnostic," *Statistical Science*, 36, 518–529.
- Wang, C., and Nydick, S. W. (2020), "On longitudinal item response theory models: A didactic," *Journal of Educational and Behavioral Statistics*, 45, 339–368.
- Watanabe, S. (2013), "A widely applicable Bayesian information criterion," *Journal of Machine Learning Research*, 14, 867–897.
- Wilson, M., Zheng, X., and McGuire, L. W. (2012), "Formulating latent growth using an explanatory item response model approach," *Journal of Applied Measurement*, 13, 1–22.

Supplement

Supplement A: Mental health data	25
Supplement B: Markov chain Monte Carlo algorithm	25
Supplement C: Details on prior and algorithm specification	27
Supplement D: Convergence diagnostics	30
Supplement E: Additional results	40

APPENDIX A: MENTAL HEALTH DATA

The following ten symptoms were used for data analysis.

1. "I was bothered by things that usually don't bother me."
2. "I had trouble keeping my mind on what I was doing."
3. "I felt depressed."
4. "I felt that everything I did was an effort."
5. "I did not feel hopeful about the future."
6. "I thought my life had been a failure."
7. "I was not happy."
8. "I talked less than usual."
9. "I felt that people dislike me."
10. "I could not get "going". "

The duration of each symptom over the last seven days was asked based on four response categories (1: rarely or none of the time (less than 1 day); 2: some or a little of the time (1-2 days); 3: occasionally or a moderate amount of time (3-4 days); 4: most or all of the time (5-7 days)). We dichotomized the responses such that response 1 became 1 and responses 2-4 became 0.

APPENDIX B: MARKOV CHAIN MONTE CARLO ALGORITHM

We approximate the posterior by combining the following Markov chain Monte Carlo steps by cycling or mixing ([Tierney, 1994](#)):

1. Sample β_j from its full conditional distribution:

$$\beta_j \sim N(m_\beta, v_\beta^2),$$

$$m_\beta = \left(\frac{1}{\sigma_\beta^2} + \sum_i \sum_t \omega_{i,j,t} \right)^{-1} \left(\sum_i \sum_t K_{i,j,t} - \sum_i \sum_t \omega_{i,j,t} \alpha_{i,t} + \sum_i \sum_t \omega_{i,j,t} \gamma d_{i,j,t} \right)$$

$$v_\beta^2 = \left(\frac{1}{\sigma_\beta^2} + \sum_i \sum_t \omega_{i,j,t} \right)^{-1},$$

where $K_{i,j,t} = Y_{i,j,t} - 1/2$, and $K_{i,j,t}/\omega_{i,j,t} \sim N(0, 1)$ with $\omega_{i,j,t} \sim \text{PG}(1, \alpha_i + \beta_j - \gamma d_{i,j,t})$, where $d_{i,j,t} = (\mathbf{a}_{i,t}, \mathbf{b}_j)$ when $T = 1$ and $d_{i,j,t} = d_{i,t} = (\mathbf{a}_{i,t}, \mathcal{J})$ when $T > 1$, where $\text{PG}(b, c)$ is a Pólya-Gamma distribution with $b > 0$ and $c \in \mathbb{R}$ (Polson et al., 2013).

2. Sample α_i from its full conditional distribution:

$$\alpha_i \sim N(m_\alpha, v_\alpha^2),$$

$$m_\alpha = \left(\frac{1}{\sigma_\alpha^2} + \sum_j \sum_t \omega_{i,j,t} \right)^{-1} \left(\sum_j \sum_t K_{i,j,t} - \sum_j \sum_t \omega_{i,j,t} \beta_{j,t} + \sum_j \sum_t \omega_{i,j,t} \gamma d_{i,j,t} \right)$$

$$v_\alpha^2 = \left(\frac{1}{\sigma_\alpha^2} + \sum_j \sum_t \omega_{i,j,t} \right)^{-1},$$

3. Sample σ_α^2 from the Inverse Gamma distribution

$$\sigma_\alpha^2 \sim \text{Inv-Gamma} \left(a_{\sigma_\alpha} + \frac{N}{2}, b_{\sigma_\alpha} + \frac{\sum_j \sum_t \alpha_i^2}{2} \right),$$

4. Sample γ from its full conditional distribution:

$$\gamma \sim \text{Half-Normal}(m_\gamma, v_\gamma^2),$$

$$m_\gamma = \left(\frac{1}{\sigma_\gamma^2} + \sum_i \sum_j \sum_t \omega_{i,t} d_{i,j,t}^2 \right)^{-1}$$

$$\times \left(\sum_i \sum_j \sum_t K_{i,j,t} d_{i,j,t} + \sum_i \sum_j \sum_t \omega_{i,j,t} \alpha_{i,t} d_{i,j,t} + \sum_i \sum_j \sum_t \omega_{i,j,t} \beta_{j,t} d_{i,j,t} \right)$$

$$v_\gamma^2 = \left(\frac{1}{\sigma_\gamma^2} + \sum_i \sum_j \sum_t \omega_{i,t} d_{i,j,t}^2 \right)^{-1}.$$

5. Propose $\lambda_{i,t}^*$ from a symmetric proposal distribution and accept the proposal with probability

$$\min \left(1, \frac{f(\lambda_{i,t}^* | \mathbf{K}, \boldsymbol{\omega}, \mathbf{A}, \mathbf{B}, \boldsymbol{\beta}, \gamma)}{f(\lambda_{i,t}^{(l)} | \mathbf{K}, \boldsymbol{\omega}, \mathbf{A}, \mathbf{B}, \boldsymbol{\beta}, \gamma)} \right).$$

6. Propose $\mathbf{a}_{i,1}^*$ from a symmetric proposal distribution and accept the proposal with probability

$$\min \left(1, \frac{f(\mathbf{a}_i^* | \mathbf{K}, \boldsymbol{\omega}, \mathbf{A}_{-i}, \mathbf{B}, \boldsymbol{\beta}, \boldsymbol{\lambda}, \gamma)}{f(\mathbf{a}_i^{(l)} | \mathbf{K}, \boldsymbol{\omega}, \mathbf{A}_{-j}, \mathbf{B}, \boldsymbol{\beta}, \boldsymbol{\lambda}, \gamma)} \right),$$

where $\mathbf{A}_{-i} = (\mathbf{a}_1, \dots, \mathbf{a}_{i-1}, \mathbf{a}_{i+1}, \dots, \mathbf{a}_n)$.

7. Propose \mathbf{b}_j^* from a symmetric proposal distribution and accept the proposal with probability

$$\min \left(1, \frac{f(\mathbf{b}_j^* | \mathbf{K}, \boldsymbol{\omega}, \mathbf{A}, \mathbf{B}_{-j}, \boldsymbol{\beta}, \boldsymbol{\lambda}, \gamma)}{f(\mathbf{b}_j^{(l)} | \mathbf{K}, \boldsymbol{\omega}, \mathbf{A}, \mathbf{B}_{-j}, \boldsymbol{\beta}, \boldsymbol{\lambda}, \gamma)} \right),$$

where $\mathbf{B}_{-j} = (\mathbf{b}_1, \dots, \mathbf{b}_{j-1}, \mathbf{b}_{j+1}, \dots, \mathbf{b}_q)$.

8. Sample $\pi_{i,t}$ from its full conditional distribution:

$$\pi_{i,t} \sim \text{Beta}(a_\pi + r_{i,t}, b_\pi + (1 - r_{i,t})),$$

where $\pi_{i,t} := \mathbb{P}(r_{i,t} = 1 | \pi_{i,t})$ and $r_{i,t} \in \{0, 1\}$ is sampled from its full conditional distribution:

$$r_{i,t} \sim \text{Bernoulli} \left(\left(1 + \frac{(1 - \pi_{i,t}) (2\pi\sigma_0^2)^{-\frac{1}{2}} \exp\left(-\frac{1}{2\sigma_0^2} (\text{logit}(\lambda_{i,t}) - \mu_0)^2\right)}{\pi_{i,t} (2\pi\sigma_1^2)^{-\frac{1}{2}} \exp\left(-\frac{1}{2\sigma_1^2} (\text{logit}(\lambda_{i,t}) - \mu_1)^2\right)} \right)^{-1} \right).$$

As proposal distributions, we use multivariate Gaussians centered at the current values of the quantities in question, with diagonal variance-covariance matrices. The variances are set to achieve acceptance rates between .3 and .4.

APPENDIX C: DETAILS ON PRIOR AND ALGORITHM SPECIFICATION

We provide additional details on the priors and Markov chain Monte Carlo algorithms used in the simulations and applications. The hyperparameters were chosen so that the priors spread most over the mass over the most plausible subsets of the parameters space.

C.1. Section 4: Simulation results.

Section 4.1

$q = 1$:

- MCMC iterations: 45,000, and burn-in period: 30,000
- Prior values: $\sigma_\beta = 5$, $a_{\sigma_\alpha} = 1$, $b_{\sigma_\alpha} = 1$, $\sigma_\gamma = 2$, $\sigma_a = 1$, $\sigma_b = 1$, $\mu_0 = -2$, $\sigma_0 = 1$, $\mu_1 = 0$, $\sigma_1 = 2$, $a_\pi = 1$, $b_\pi = 1$.

Standard deviations of the Gaussian proposal distributions, centered at the current values of the parameters: 1.7 ($\mathbf{a}_{1,t}$); .6 (\mathbf{b}_j); and 5 ($\lambda_{i,t}$).

$q = 2$:

- MCMC iterations: 65,000, and burn-in period: 50,000
- Prior values: $\sigma_\beta = 5$, $a_{\sigma_\alpha} = 1$, $b_{\sigma_\alpha} = 1$, $\sigma_\gamma = 2$, $\sigma_a = 1$, $\sigma_b = 1$, $\mu_0 = -2$, $\sigma_0 = 1$, $\mu_1 = 0$, $\sigma_1 = 2$, $a_\pi = 1$, $b_\pi = 1$.

Standard deviations of the Gaussian proposal distributions, centered at the current values of the parameters: 1.4 ($\mathbf{a}_{1,t}$); .8 (\mathbf{b}_j); and 5 ($\lambda_{i,t}$).

$q = 3$:

- MCMC iterations: 85,000, and burn-in period: 70,000
- Prior values: $\sigma_\beta = 5$, $a_{\sigma_\alpha} = 1$, $b_{\sigma_\alpha} = 1$, $\sigma_\gamma = 2$, $\sigma_a = 1$, $\sigma_b = 1$, $\mu_0 = -2$, $\sigma_0 = 1$, $\mu_1 = 0$, $\sigma_1 = 2$, $a_\pi = 1$, $b_\pi = 1$.

Standard deviations of the Gaussian proposal distributions, centered at the current values of the parameters: 1 ($\mathbf{a}_{1,t}$); .6 (\mathbf{b}_j); and 5 ($\lambda_{i,t}$).

$q = 4$:

- MCMC iterations: 85,000, and burn-in period: 70,000
- Prior values: $\sigma_\beta = 5$, $a_{\sigma_\alpha} = 1$, $b_{\sigma_\alpha} = 1$, $\sigma_\gamma = 2$, $\sigma_a = 1$, $\sigma_b = 1$, $\mu_0 = -2$, $\sigma_0 = 1$, $\mu_1 = 0$, $\sigma_1 = 2$, $a_\pi = 1$, $b_\pi = 1$.

Standard deviations of the Gaussian proposal distributions, centered at the current values of the parameters: .9 ($\mathbf{a}_{1,t}$); .3 (\mathbf{b}_j); and 5 ($\lambda_{i,t}$).

Section 4.2:

$q = 1$:

- MCMC iterations: 45,000, and burn-in period: 30,000
- Prior values: $\sigma_\beta = 5$, $a_{\sigma_\alpha} = 1$, $b_{\sigma_\alpha} = 1$, $\sigma_\gamma = 2$, $\sigma_a = 1$, $\sigma_b = 1$, $\mu_0 = -2$, $\sigma_0 = 1$, $\mu_1 = 0$, $\sigma_1 = 2$, $a_\pi = 1$, $b_\pi = 1$.

Standard deviations of the Gaussian proposal distributions, centered at the current values of the parameters: 1.8 ($\mathbf{a}_{1,t}$); .1 (\mathbf{b}_j); and 5 ($\lambda_{i,t}$).

$q = 2$:

- MCMC iterations: 65,000, and burn-in period: 50,000
- Prior values: $\sigma_\beta = 5$, $a_{\sigma_\alpha} = 1$, $b_{\sigma_\alpha} = 1$, $\sigma_\gamma = 2$, $\sigma_a = 1$, $\sigma_b = 1$, $\mu_0 = -2$, $\sigma_0 = 1$, $\mu_1 = 0$, $\sigma_1 = 2$, $a_\pi = 1$, $b_\pi = 1$.

Standard deviations of the Gaussian proposal distributions, centered at the current values of the parameters: 1.4 ($\mathbf{a}_{1,t}$); .3 (\mathbf{b}_j); and 5 ($\lambda_{i,t}$).

$q = 3$:

- MCMC iterations: 85,000, and burn-in period: 70,000
- Prior values: $\sigma_\beta = 5$, $a_{\sigma_\alpha} = 1$, $b_{\sigma_\alpha} = 1$, $\sigma_\gamma = 2$, $\sigma_a = 1$, $\sigma_b = 1$, $\mu_0 = -2$, $\sigma_0 = 1$, $\mu_1 = 0$, $\sigma_1 = 2$, $a_\pi = 1$, $b_\pi = 1$.

Standard deviations of the Gaussian proposal distributions, centered at the current values of the parameters: .8 ($\mathbf{a}_{1,t}$); .15 (\mathbf{b}_j); and 5 ($\lambda_{i,t}$).

$q = 4$:

- MCMC iterations: 85,000, and burn-in period: 70,000
- Prior values: $\sigma_\beta = 5$, $a_{\sigma_\alpha} = 1$, $b_{\sigma_\alpha} = 1$, $\sigma_\gamma = 2$, $\sigma_a = 1$, $\sigma_b = 1$, $\mu_0 = -2$, $\sigma_0 = 1$, $\mu_1 = 0$, $\sigma_1 = 2$, $a_\pi = 1$, $b_\pi = 1$.

Standard deviations of the Gaussian proposal distributions, centered at the current values of the parameters: .7 ($\mathbf{a}_{1,t}$); .08 (\mathbf{b}_j); and 5 ($\lambda_{i,t}$).

C.2. Section 6: Application: online educational assessments.

Section 6.2:

$q = 1$:

- MCMC iterations: 45,000, and burn-in period: 30,000
- Prior values: $\sigma_\beta = 5$, $a_{\sigma_\alpha} = 1$, $b_{\sigma_\alpha} = 1$, $\sigma_\gamma = 2$, $\sigma_a = 1$, $\sigma_b = 1$, $\mu_0 = -2$, $\sigma_0 = 1$, $\mu_1 = 0$, $\sigma_1 = 2$, $a_\pi = 1$, $b_\pi = 1$.

Standard deviations of the Gaussian proposal distributions, centered at the current values of the parameters: 1.4 ($\mathbf{a}_{1,t}$); .2 (\mathbf{b}_j); and 6 ($\lambda_{i,t}$).

$q = 2$:

- MCMC iterations: 45,000, and burn-in period: 30,000
- Prior values: $\sigma_\beta = 5$, $a_{\sigma_\alpha} = 1$, $b_{\sigma_\alpha} = 1$, $\sigma_\gamma = 2$, $\sigma_a = 1$, $\sigma_b = 1$, $\mu_0 = -2$, $\sigma_0 = 1$, $\mu_1 = 0$, $\sigma_1 = 2$, $a_\pi = 1$, $b_\pi = 1$.

Standard deviations of the Gaussian proposal distributions, centered at the current values of the parameters: .8 ($\mathbf{a}_{1,t}$); .1 (\mathbf{b}_j); and 5 ($\lambda_{i,t}$).

$q = 3$:

- MCMC iterations: 65,000, and burn-in period: 50,000
- Prior values: $\sigma_\beta = 5$, $a_{\sigma_\alpha} = 1$, $b_{\sigma_\alpha} = 1$, $\sigma_\gamma = 2$, $\sigma_a = 1$, $\sigma_b = 1$, $\mu_0 = -2$, $\sigma_0 = 1$, $\mu_1 = 0$, $\sigma_1 = 2$, $a_\pi = 1$, $b_\pi = 1$.

Standard deviations of the Gaussian proposal distributions, centered at the current values of the parameters: .6 ($\mathbf{a}_{1,t}$); .1 (\mathbf{b}_j); and 5 ($\lambda_{i,t}$).

$q = 4$:

- MCMC iterations: 65,000, and burn-in period: 50,000
- Prior values: $\sigma_\beta = 5$, $a_{\sigma_\alpha} = 1$, $b_{\sigma_\alpha} = 1$, $\sigma_\gamma = 2$, $\sigma_a = 1$, $\sigma_b = 1$, $\mu_0 = -2$, $\sigma_0 = 1$, $\mu_1 = 0$, $\sigma_1 = 2$, $a_\pi = 1$, $b_\pi = 1$.

Standard deviations of the Gaussian proposal distributions, centered at the current values of the parameters: .6 ($\mathbf{a}_{1,t}$); .07 (\mathbf{b}_j); and 5 ($\lambda_{i,t}$).

C.3. Section 5: Application: mental health.

Section 5.2:

$q = 1$:

- MCMC iterations: 65,000, and burn-in period: 50,000
- Prior values: $\sigma_\beta = 5$, $a_{\sigma_\alpha} = 1$, $b_{\sigma_\alpha} = 1$, $\sigma_\gamma = 2$, $\sigma_a = 1$, $\sigma_b = 1$, $\mu_0 = -2$, $\sigma_0 = 1$, $\mu_1 = 0$, $\sigma_1 = 2$, $a_\pi = 1$, $b_\pi = 1$.

Standard deviations of the Gaussian proposal distributions, centered at the current values of the parameters: 1.4 ($\mathbf{a}_{1,t}$); .2 (\mathbf{b}_j); and 6 ($\lambda_{i,t}$).

$q = 2$:

- MCMC iterations: 65,000, and burn-in period: 50,000

- Prior values: $\sigma_\beta = 5$, $a_{\sigma_\alpha} = 1$, $b_{\sigma_\alpha} = 1$, $\sigma_\gamma = 2$, $\sigma_a = 1$, $\sigma_b = 1$, $\mu_0 = -2$, $\sigma_0 = 1$, $\mu_1 = 0$, $\sigma_1 = 2$, $a_\pi = 1$, $b_\pi = 1$.

Standard deviations of the Gaussian proposal distributions, centered at the current values of the parameters: .7 ($\mathbf{a}_{1,t}$); .1 (\mathbf{b}_j); and 5 ($\lambda_{i,t}$).

$q = 3$:

- MCMC iterations: 65,000, and burn-in period: 50,000
- Prior values: $\sigma_\beta = 5$, $a_{\sigma_\alpha} = 1$, $b_{\sigma_\alpha} = 1$, $\sigma_\gamma = 2$, $\sigma_a = 1$, $\sigma_b = 1$, $\mu_0 = -2$, $\sigma_0 = 1$, $\mu_1 = 0$, $\sigma_1 = 2$, $a_\pi = 1$, $b_\pi = 1$.

Standard deviations of the Gaussian proposal distributions, centered at the current values of the parameters: .8 ($\mathbf{a}_{1,t}$); .1 (\mathbf{b}_j); and 5 ($\lambda_{i,t}$).

$q = 4$:

- MCMC iterations: 200,000, and burn-in period: 185,000
- Prior values: $\sigma_\beta = 5$, $a_{\sigma_\alpha} = 1$, $b_{\sigma_\alpha} = 1$, $\sigma_\gamma = 2$, $\sigma_a = 1$, $\sigma_b = 1$, $\mu_0 = -2$, $\sigma_0 = 1$, $\mu_1 = 0$, $\sigma_1 = 2$, $a_\pi = 1$, $b_\pi = 1$.

Standard deviations of the Gaussian proposal distributions, centered at the current values of the parameters: .8 ($\mathbf{a}_{1,t}$); .1 (\mathbf{b}_j); and 5 ($\lambda_{i,t}$).

APPENDIX D: CONVERGENCE DIAGNOSTICS

To detect non-convergence of the Markov chains used for approximating the posterior, we use

- trace plots of parameters (Supplement [D.1](#));
- the multivariate Gelman-Rubin potential scale reduction factor of [Vats and Knudson \(2021\)](#), which can be viewed as a stable version of the multivariate Gelman-Rubin convergence diagnostic and comes with a convergence criterion (Supplement [D.2](#)).

D.1. Trace plots.

D.1.1. *Section 6: Application: online educational assessments.*

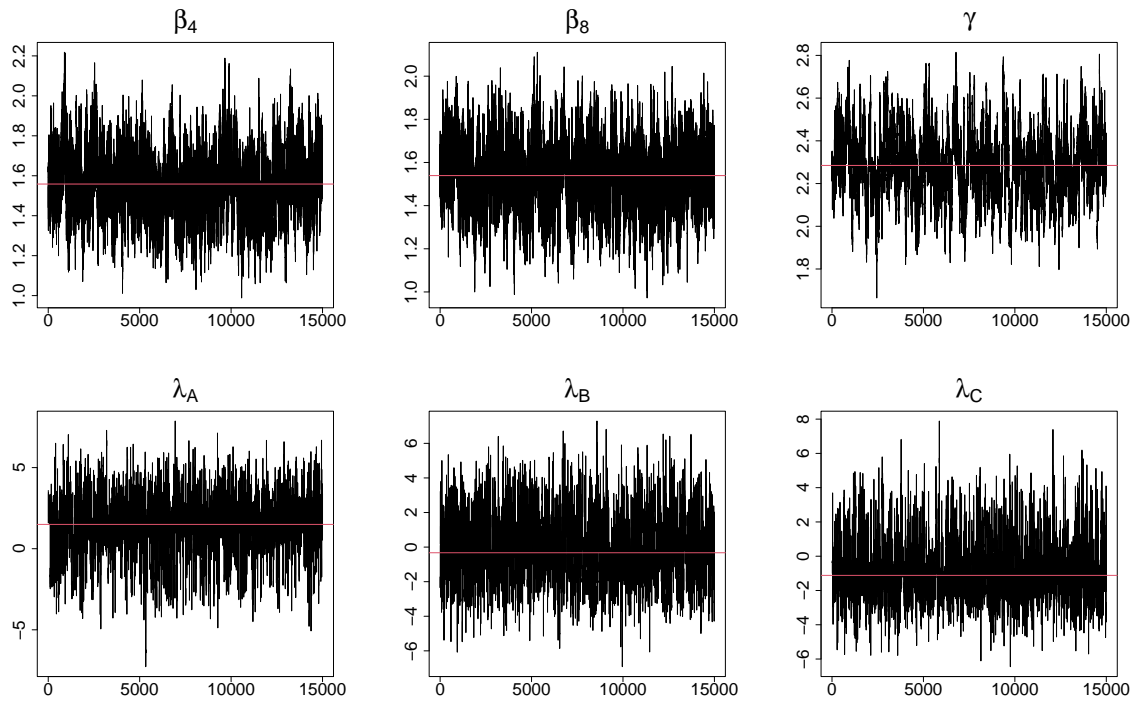


FIG 14. Trace plots of select parameters from the latent process model with $q = 1$ in Section 6.2. The red-colored horizontal lines indicate posterior medians.

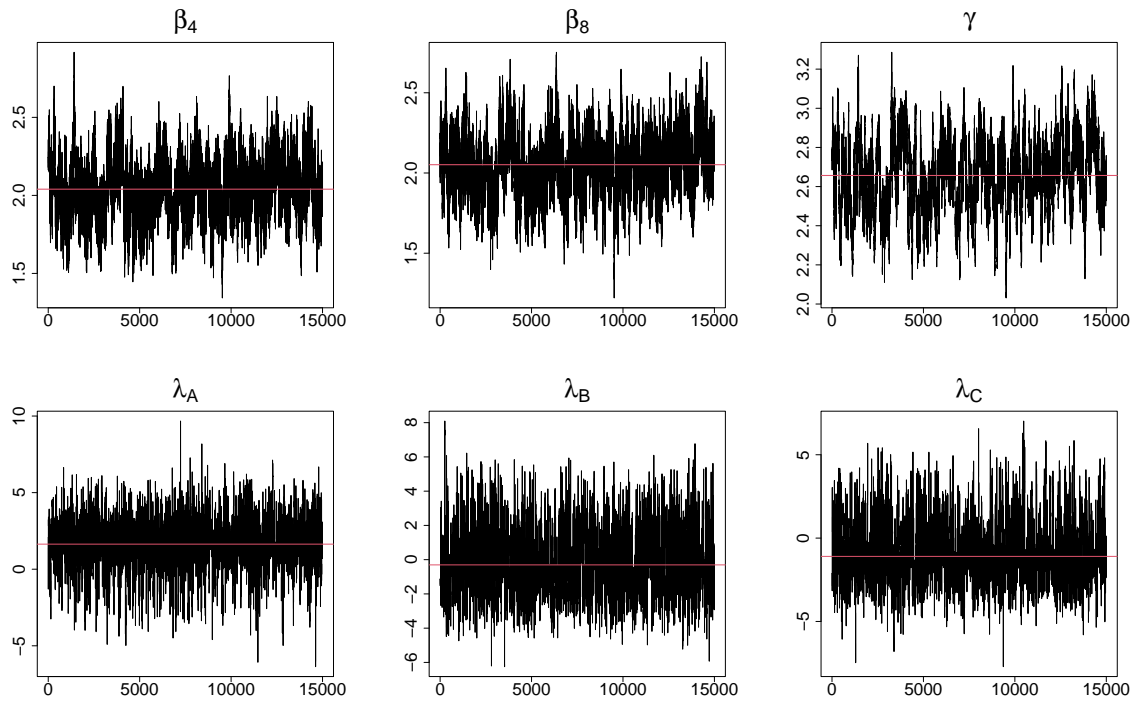


FIG 15. Trace plots of select parameters from the latent process model with $q = 2$ in Section 6.2. The red-colored horizontal lines indicate posterior medians.

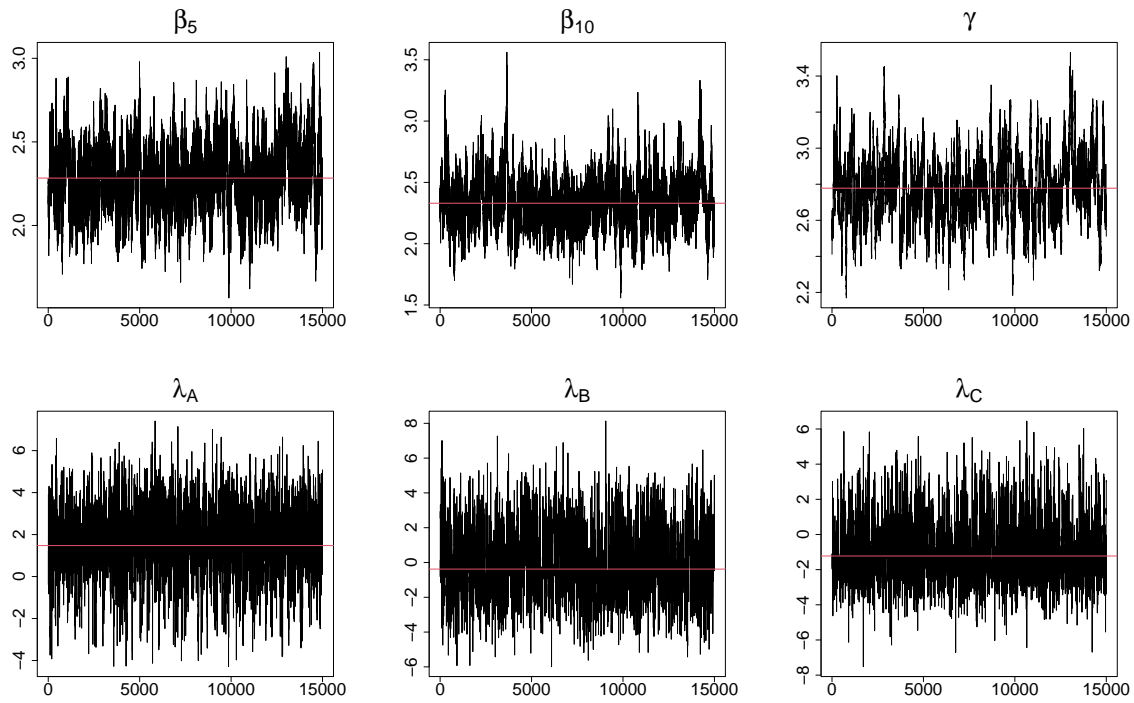


FIG 16. Trace plots of select parameters from the latent process model with $q = 3$ in Section 6.2. The red-colored horizontal lines indicate posterior medians.

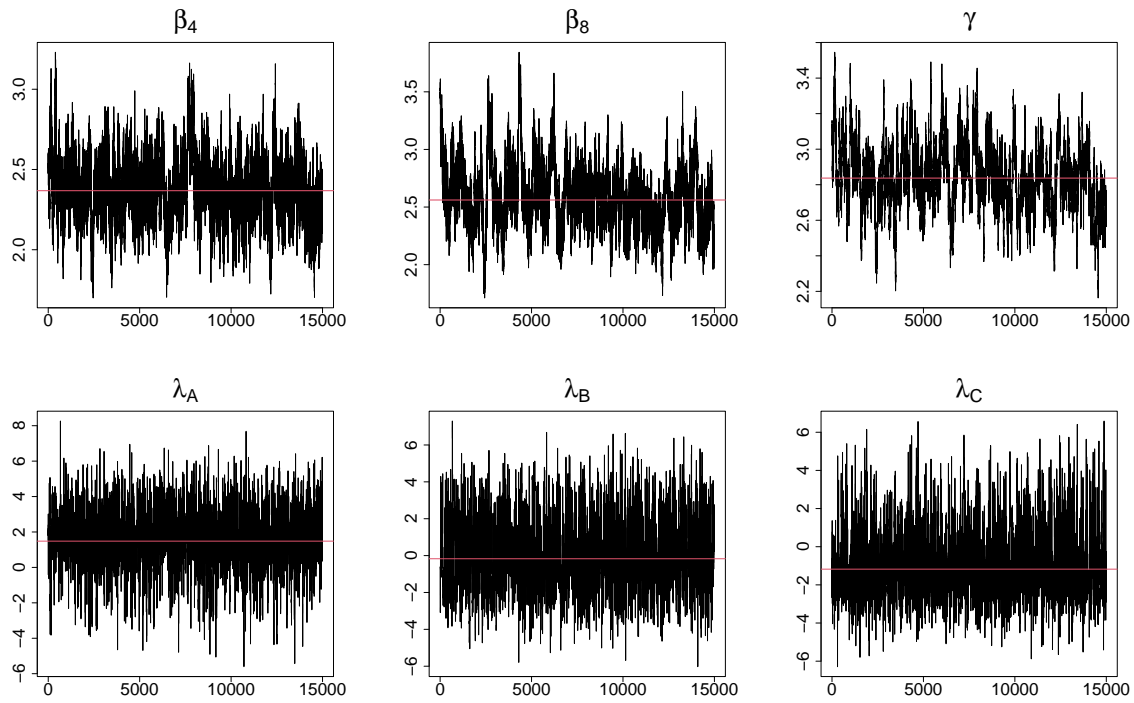


FIG 17. Trace plots of select parameters from the latent process model with $q = 4$ in Section 6.2. The red-colored horizontal lines indicate posterior medians.

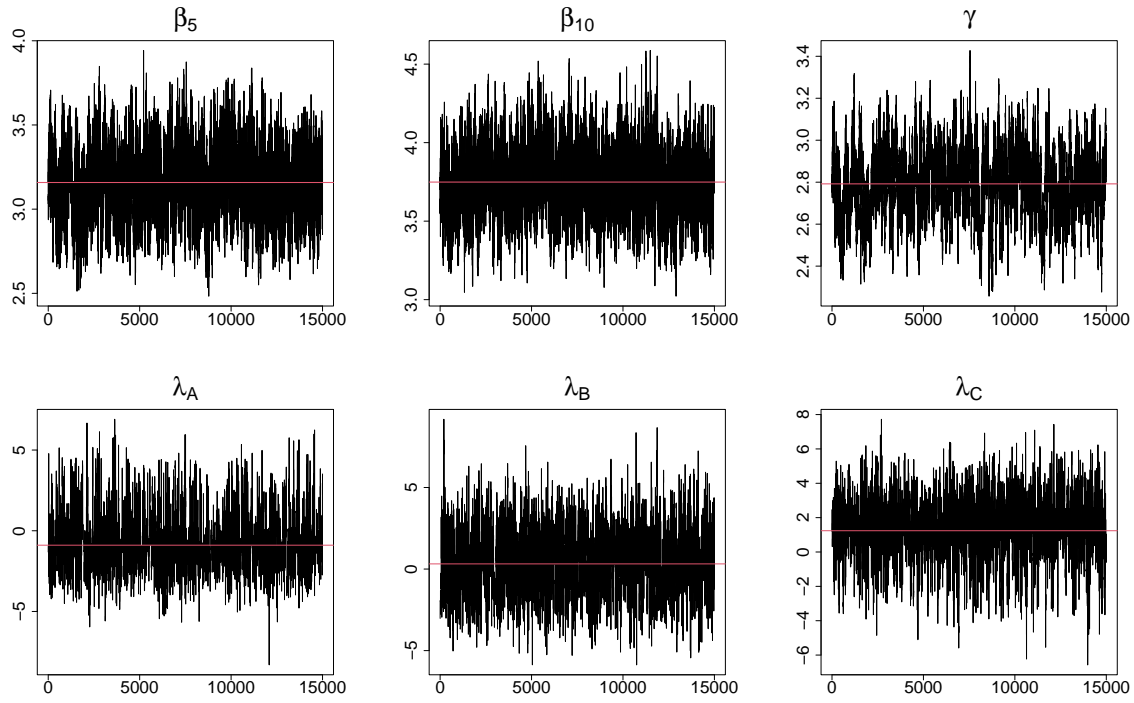


FIG 18. Trace plots of select parameters from the latent process model with $q = 1$ in Section 5.2. The red-colored horizontal lines indicate posterior medians.

D.1.2. Section 5: Application: mental health.

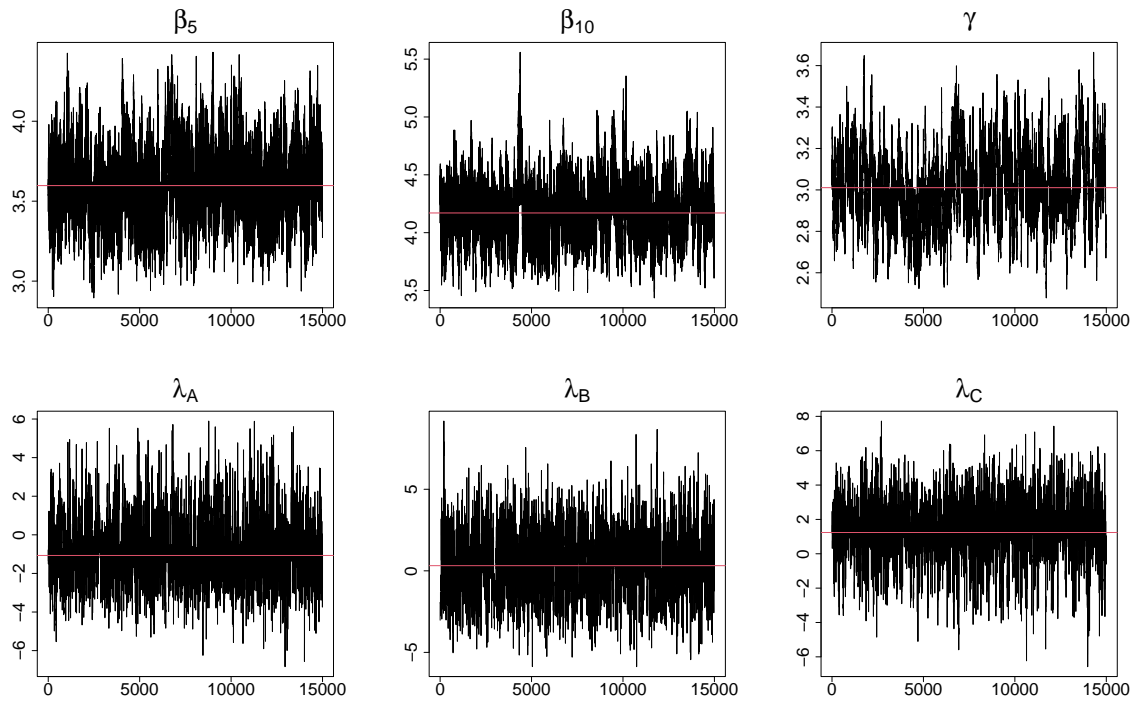


FIG 19. Trace plots of select parameters from the latent process model with $q = 2$ in Section 5.2. The red-colored horizontal lines indicate posterior medians.

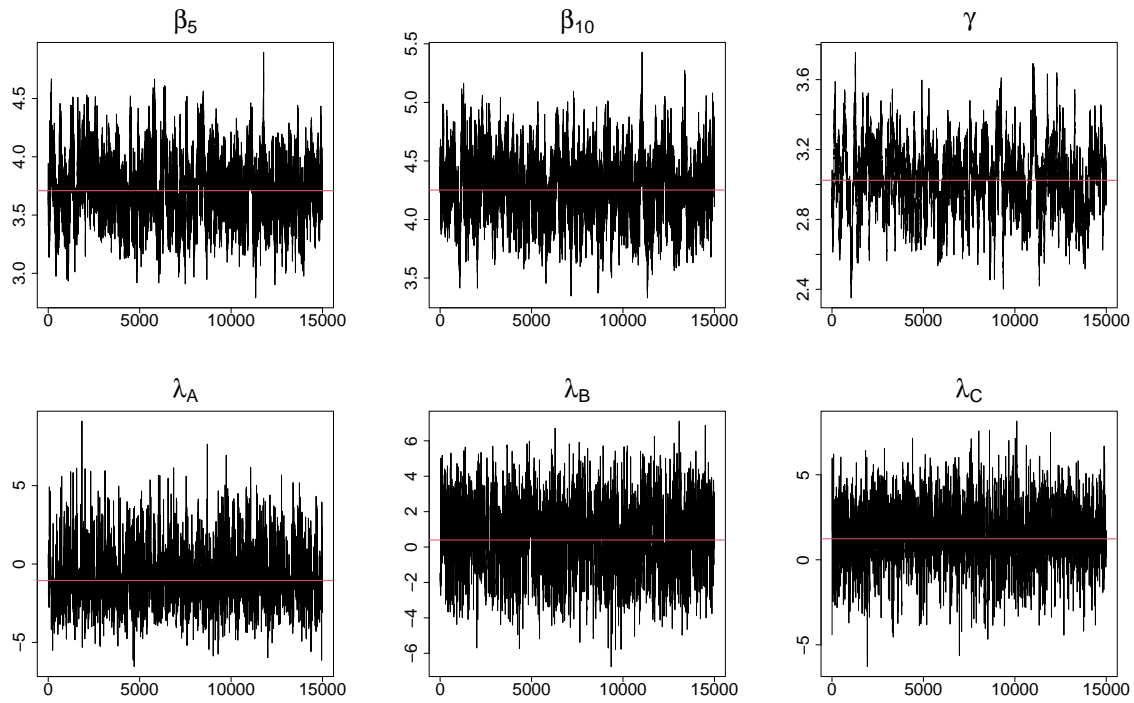


FIG 20. Trace plots of select parameters from the latent process model with $q = 3$ in Section 5.2. The red-colored horizontal lines indicate posterior medians.

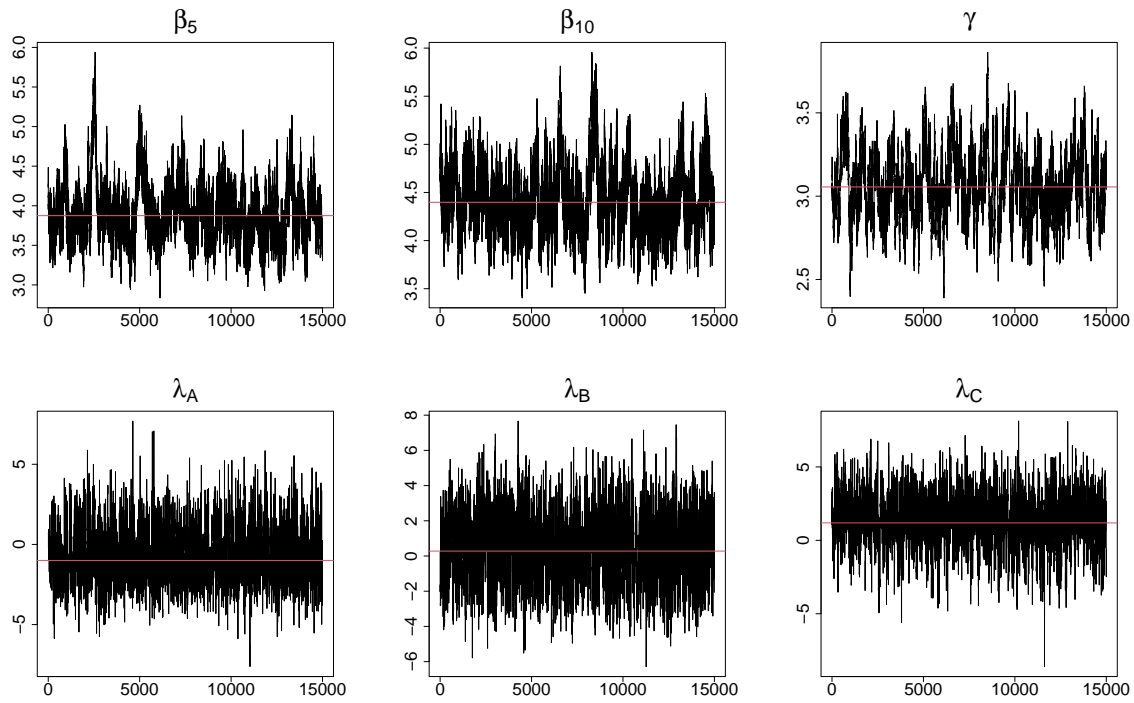


FIG 21. Trace plots of select parameters from the latent process model with $q = 4$ in Section 5.2. The red-colored horizontal lines indicate posterior medians.

D.2. Multivariate Gelman-Rubin Potential Scale Reduction Factor. As a convergence diagnostic, we use the multivariate Gelman-Rubin potential scale reduction factor (PSRF) stated in Equation (10) of Vats and Knudson (2021, p. 522) (see also Vats and Flegal, 2021). The multivariate Gelman-Rubin PSRF can be viewed as a stable version of the Gelman-Rubin convergence diagnostic (Gelman and Rubin, 1992) and has the additional advantage of providing a principled approach for determining whether a Markov chain did not converge. We use the PSRF cutoff suggested by Vats and Knudson in Example 1 on page 523 of Vats and Knudson (2021). If the PSRF exceeds the PSRF cutoff, there is reason to believe that one or more Markov chains did not converge and more samples are required. According to Table 7, the multivariate Gelman-Rubin PSRF is less than the PSRF cutoff in all applications, based on 5 Markov chains with starting values chosen at random, so there are no signs of non-convergence.

	# parameters	PSRF				PSRF cutoff
		$q = 1$	$q = 2$	$q = 3$	$q = 4$	
Section 6.2	852	1.000227	1.000214	1.000208	1.000208	1.000342
Section 5.2	526	1.000303	1.000268	1.000276	1.000280	1.000336

TABLE 7

The multivariate Gelman-Rubin PSRF and PSRF cutoff in Sections 6.2 and 5.2. The results are based on 5 Markov chains with starting values chosen at random.

APPENDIX E: ADDITIONAL RESULTS

	Minimum	25% Percentile	Median	Mean	75% Percentile	Maximum
<i>q</i> = 1:						
λ	0.133	0.330	0.477	0.472	0.606	0.886
α	-0.985	-0.593	-0.237	-0.039	0.339	1.911
β	-0.703	0.637	1.327	1.123	1.721	2.529
<i>q</i> = 2:						
λ	0.099	0.290	0.456	0.448	0.608	0.881
α	-1.042	-0.584	-0.229	-0.033	0.362	1.847
β	-0.263	1.152	1.810	1.613	2.215	3.038
<i>q</i> = 3:						
λ	0.095	0.276	0.444	0.442	0.602	0.873
α	-1.095	-0.577	-0.213	-0.032	0.348	1.857
β	-0.022	1.474	2.045	1.876	2.484	3.294
<i>q</i> = 4:						
λ	0.099	0.298	0.453	0.449	0.593	0.878
α	-1.024	-0.570	-0.231	-0.0362	0.309	1.834
β	0.071	1.633	2.171	2.029	2.694	3.466

TABLE 8

Summary of the posterior medians of λ , θ , and β

from the latent process model for Application: online educational assessments in Section 6.2. Pearson correlations between the posterior medians of λ across models with different latent space dimensions ranged from .990 to .994 and Spearman rank-order correlations ranged from .991 to .995.

	Median	2.5 Percentile	97.5 Percentile
<i>q</i> = 1:			
γ	2.284	1.978	2.605
σ_α	1.054	0.962	1.156
<i>q</i> = 2:			
γ	2.656	2.303	3.003
σ_α	1.038	0.948	1.138
<i>q</i> = 3:			
γ	2.777	2.429	3.169
σ_α	1.035	0.943	1.134
<i>q</i> = 4:			
γ	2.837	2.470	3.234
σ_α	1.031	0.941	1.131

TABLE 9

Summary (posterior median and 95% credible intervals) of γ and σ_α from the latent process model for Application: online educational assessments in Section 6.2

	Minimum	25% Percentile	Median	Mean	75% Percentile	Maximum
<i>q</i> = 1:						
λ	0.069	0.295	0.554	0.506	0.701	0.918
α	-1.050	-0.504	-0.104	0.002	0.455	1.075
β	1.894	2.360	3.066	2.983	3.606	3.939
<i>q</i> = 2:						
λ	0.062	0.245	0.569	0.495	0.709	0.914
α	-1.213	-0.523	0.015	0.005	0.553	1.131
β	2.283	2.766	3.493	3.410	4.023	4.395
<i>q</i> = 3:						
λ	0.062	0.275	0.565	0.502	0.704	0.907
α	-1.274	-0.589	0.023	0.001	0.594	1.197
β	2.266	2.830	3.568	3.499	4.142	4.556
<i>q</i> = 4:						
λ	0.069	0.304	0.552	0.511	0.706	0.905
α	-1.321	-0.641	0.024	-0.005	0.607	1.204
β	2.256	3.138	3.801	3.715	4.390	4.797

TABLE 10

Summary of the posterior medians of λ , θ , and β

from the latent process model for Application: mental health in Section 5.2. Pearson correlations between the posterior medians of λ across models with different latent space dimensions ranged from .988 to .996 and Spearman rank-order correlations ranged from .988 to .993.

	Median	2.5 Percentile	97.5 Percentile
<i>q</i> = 1:			
γ	2.791	2.456	3.109
σ_α	1.018	0.903	1.147
<i>q</i> = 2:			
γ	3.010	2.683	3.385
σ_α	1.031	0.916	1.162
<i>q</i> = 3:			
γ	3.023	2.646	3.407
σ_α	1.051	0.935	1.181
<i>q</i> = 4:			
γ	3.055	2.688	3.477
σ_α	1.065	0.948	1.195

TABLE 11

Summary (posterior median and 95% credible intervals) of γ and σ_α from the latent process model for Application: mental health in Section 5.2.

MINJEONG JEON
 DEPARTMENT OF EDUCATION
 UNIVERSITY OF CALIFORNIA, LOS ANGELES
 MOORE HALL 3141
 405 HILGARD AVENUE
 LOS ANGELES, CA 90095-1521
 E-MAIL: MJJEON@G.UCLA.EDU

MICHAEL SCHWEINBERGER
 DEPARTMENT OF STATISTICS
 PENN STATE UNIVERSITY
 326 THOMAS BUILDING
 UNIVERSITY PARK, PA 16802
 E-MAIL: MUS47@PSU.EDU